

VIBRATIONAL RELAXATION
TIME STUDIES ON CARBON MONOXIDE
BY THE INFRARED SPECTROPHONE METHOD

by

WALTER DENNY JONES

A THESIS

submitted to

OREGON STATE COLLEGE

in partial fulfillment of
the requirements for the
degree of

DOCTOR OF PHILOSOPHY

June 1958

APPROVED:



Professor of Chemistry

In Charge of Major



Chairman of Department of Chemistry



Chairman of School Graduate Committee



Dean of Graduate School

Date thesis is presented October 25, 1957

Typed by Francine Reeves

ACKNOWLEDGMENT

To Dr. J. C. Decius I extend my deepest gratitude. He has been considerably more than a very able major professor to me throughout my career at this institution, extending his friendship, advice, and philosophy in a highly satisfying relationship.

I wish to thank all those who have helped make life so pleasant and given the constructive criticism that is of so much value to the researcher. In particular I include fellow graduate students and members of the faculty with whom I have been associated.

I give my thanks to Dr. D. F. Swineheart of the University of Oregon and to Mrs. S. Y. Wu and Mr. John G. Skinner of Oregon State College for the mass-spectrometric analysis.

This work was supported in part by the Office of Naval Research under Contract Nonr-974(00).

TABLE OF CONTENTS

	Page
INTRODUCTION	1
THEORY	3
EXPERIMENTAL METHODS	12
ELEMENTARY SPECTROPHONE PROCESSES	15
EXPERIMENTAL TECHNIQUE	30
EXPERIMENTAL RESULTS	41
Carbon Monoxide-Hydrogen Mixtures	41
Carbon Monoxide-Helium Mixtures	47
Carbon Monoxide-Neon Mixture	47
Carbon Monoxide-Argon Mixture	50
The Effect of Mass on the Relaxation Time	50
CONCLUSIONS	55
BIBLIOGRAPHY	60
APPENDIX I	64
APPENDIX II	68
APPENDIX III	74
APPENDIX IV	77

LIST OF TABLES

	Page
I	Vibrational Relaxation Measurements on Hydrogen-Carbon Monoxide Mixtures 42
II	Corrected Values of $\Delta\tau$ and $1/\Delta\tau$ for Hydrogen-Carbon Monoxide Mixtures 45
III	Vibrational Relaxation Data of Carbon Monoxide-Helium Mixtures 48
IV	Experimental Results, Carbon Monoxide- Neon Mixture 49
V	Experimental Results, Carbon Monoxide- Argon Mixture 51
VI	Relaxation Time as a Function of Reduced Mass 52
VII	Relaxation Time and Probability of Deexcitation on Collision for Various Carbon Monoxide Mixtures 56
VIII	Theoretical Calculation of Relaxation Times for Carbon Monoxide Mixtures 65
IX	Evaluation of Quantities Found in Inequalities in Development of Theory 66
X	Calculation of $\tau = \frac{1}{\omega \tan \omega t}$ and $\tau = \frac{\pi}{2\omega} - t$. 75

LIST OF FIGURES

		Page
I	Block Diagram of Spectrophone	31
II	Spectrophone Cell	34
III	Schematic Diagram of Gas Handling Apparatus .	36
IV	Gas Handling System	37
V	Carbon Monoxide-Hydrogen: $\frac{1}{\Delta t}$ vs. $\frac{1}{p}$	43
VI	Carbon Monoxide-Hydrogen: $\frac{1}{\Delta \tau}$ vs. $\frac{1}{p}$ (Corrected Values)	46
VII	Effect of Mass on the Relaxation Time of Carbon Monoxide	53
VIII	Comparison of $\tau = \frac{1}{\omega \tan \omega t}$ with $\tau = \frac{\pi}{2\omega} - t$	76

VIBRATIONAL RELAXATION
TIME STUDIES ON CARBON MONOXIDE
BY THE INFRARED SPECTROPHONE METHOD

INTRODUCTION

The observation of dispersion in the velocity of sound at supersonic frequencies led to the postulation of a vibrational relaxation time of the order of 10^{-5} seconds by Herzfeld and Rice (16) in 1928 and again by Kneser in 1931. Since that time much interest has been shown in this phenomenon both in theoretical interpretation and in methods of measurement. It plays a particular role in the study of rapid, non-equilibrium processes such as detonation, shock waves, and the kinetics of jet propulsion. In a previous thesis, Turrell (38) gives an excellent discussion of the historical background concerning vibrational relaxation. Other reviews including detailed bibliographies have been prepared by Richards (26) and Richardson (27).

It is universally assumed that the relaxation mechanism is a process involving molecular collisions indicating a pressure dependency. The mass of data to date supports this assumption and in particular van Itterbeek and Mariens (39) measured the pressure dependence and found it in agreement with the assumption of a collision process. Various investigators have developed theories, both classical and quantum-mechanical, based on this assumption, leading to very similar expressions for the probability

of energy transfer. However, in recent years Amme and Legvold (1), Rossing and Legvold (28), and Fogg, Hanks, and Lambert (13) in studies on halogen-substituted methanes found that a theory based on an energy of excitation fitted their data better. Such a theory predicts that there is no mass dependence in the relaxation process, whereas previous theory predicted a very large mass effect, particularly in the case of a high vibrational frequency. An excellent test of the applicability of the two theories then would be the measurement of the mass dependence of the relaxation time of a high frequency vibrational mode. Carbon monoxide with a single frequency of 2160 cm^{-1} satisfies this condition.

THEORY

The earliest attempt at a quantitative theoretical determination of vibrational relaxation times was made by Zener in 1931 (41, 42). He discussed a simple one dimensional model along purely classical lines. A more detailed classical discussion was prepared by Landau and Teller (22) in 1936. They found that the probability of excitation during a collision was proportional to an exponential term of the form

$$P_{0 \rightarrow 1} \sim \exp \left\{ - \sqrt[3]{\frac{27 \pi^2 a^2 \nu^2 M}{2kT}} \right\}$$

Here $P_{0 \rightarrow 1}$ is the probability of a molecule being excited from its ground state to its first vibrational level, a is a distance parameter based on the range of the interaction potential, ν is the vibrational frequency, M is the reduced mass of the collision $\left(\frac{M_A M_B}{M_A + M_B} \right)$, k is Boltzmann's constant, and T is the absolute temperature.

For many years, this was the most satisfactory expression available. Other investigators presented an analysis of the problem but none gave as tractable an expression for making estimates of vibrational amplitudes without the use of a computing machine. Bourgin (4) made a three dimensional analysis, comparing it with Kneser's work, which he considered a special case of his treatment.

More recently Curtis and Adler (6) published a quantum mechanical discussion of collisions with diatomic molecules, deriving scattering coefficients for the process. Other discussions have been carried out recently by Widom and S. H. Bauer (40) and Ernest Bauer (2).

Of more practical importance, however, is the derivation by means of quantum mechanics of an expression that readily permits an estimation of relaxation times. This is the work of Schwartz, Slawsky, and Herzfeld (30) in 1952. Using the same simple model of Landau and Teller, they derived an exponential behavior identical to that of the classical theory. Explicitly, their results are

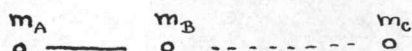
$$P_{1 \rightarrow 0} = V_i^2 (1 \rightarrow 0) V_r^2$$

$V_i (1 \rightarrow 0)$ is the matrix element for a decrease in vibrational energy from the first level to the ground state while V_r is the matrix element for an equivalent increase in translational energy. Further

$$V_i (1 \rightarrow 0) = -\alpha A_n \left[\frac{h}{8\pi^2 \mu \nu_n} \right]^{\frac{1}{2}}$$

α is a parameter representing the range of forces in the collision process. It is found by fitting a potential energy curve of the form $V = V_0 e^{-\alpha r}$ to the repulsive portion of the Lennard-Jones potential. A_n is the coefficient of the nth normal coordinate in the expansion

of the distance from the colliding molecule to the interacting atom in terms of the intermolecular distance and the normal coordinates of the molecule undergoing transition. Thus, for the simple model of a monatomic molecule colliding along its axis with a diatomic molecule, $r = r_0 + Aq$, q the vibrational normal coordinate. In this case $A = \frac{\mu}{m_B}$



More complex expressions for A_n arise for molecules of more than two atoms.

h = Planck's constant

$$M = \text{reduced mass} = \frac{M_A M_B}{M_A + M_B}$$

ν_n = vibrational frequency of the n th normal coordinate

A precise evaluation of the factor V_r^2 is not available because of the inability to evaluate the necessary integral in closed form. Assuming that $\exp \left\{ \frac{4 \pi^2 M \nu_0}{\alpha h} \right\} \gg 1$ this integral takes the approximate form

$$V_r^2 = A \int_0^\infty v_0^3 \exp. \left\{ \frac{4 \pi^2 M (\nu_0 - \nu_f)}{\alpha h} - \frac{M \nu_0^2}{2kT} \right\} dv_0$$

where A is a constant; M is the reduced collision mass, $M = \frac{(M_A + M_B) M_C}{M_A + M_B + M_C}$; and ΔE = one quantum of vibrational energy. The integrand takes on a maximum value for some ν_0 , ν_0^* , and it is in this region that the principal

contribution to the integral is made. This occurs very nearly at the maximum value of the exponential term, and evaluation of this maximum value leads us to the approximate solution of the integral

$$V_r^2 = A' \sigma^{3/2} e^{-\sigma} \quad A' \text{ a constant}$$

$$\sigma = \text{minimum value of } \frac{4\pi^2 M}{\alpha h} (v_f - v_o) + \frac{M}{2kT} v_o^2$$

v_o^* is found by expanding $v_f = \sqrt{v_o^2 - \frac{2\Delta E}{M}}$

$$v_f = v_o \left\{ 1 + \frac{\Delta E}{M v_o^2} - \frac{(\Delta E)^2}{2M^2 v_o^4} + \dots \right\}$$

giving for the exponent to be minimized

$$\frac{M}{2kT} v_o^2 + \frac{4\pi^2}{\alpha h} \frac{\Delta E}{v_o} - \frac{2\pi^2 (\Delta E)^2}{\alpha h M v_o^3}$$

In order that this expansion be valid we must have

$$\frac{M}{2} v_f^{*2} \gg \Delta E \quad \text{and} \quad \frac{M}{2} v_o^{*2} \gg \Delta E.$$

$$\text{This gives } v_o^* = \left(\frac{4\pi^2 kT \Delta E}{\alpha^* h M} \right)^{1/3} - \frac{\Delta E}{2M} \left(\frac{4\pi^2 kT \Delta E}{\alpha^* h M} \right)^{-1/3}$$

and for the transition probability

$$\begin{aligned} V_r^2 &= 0.39 \left(\frac{8\pi^3 M \Delta E}{\alpha^2 h^2} \right)^2 \sigma^{3/2} e^{-\sigma} \\ &= 3 \left(\frac{2\pi^4 (\Delta E)^2 M}{\alpha^2 h^2 kT} \right)^{1/3} - \frac{\Delta E}{2kT} \end{aligned}$$

The exponential $e^{-\sigma}$ is the most significant term in this expression and an investigation of its dependence should describe fairly well the dependence of the probability of deexcitation. In general $3 \left(\frac{2 \pi^4 (\Delta E)^2 M}{\alpha^2 h^2 kT} \right)^{1/3} > \frac{\Delta E}{2kT}$ and

the latter term can be neglected in view of the approximate nature of this discussion. We observe, then, that approximately $\sigma = C \frac{\omega^{2/3} M^{1/3}}{T^{1/3}}$, C a constant, and

$-\sigma = D + \log P_{1 \rightarrow 0}$, D very nearly a constant.

In Appendix I the relaxation times of the carbon monoxide mixtures under study have been calculated by the Schwartz - Slawsky - Herzfeld theory. Also, the values of v_0^* have been calculated to test the validity of the approximations made. It is observed that the approximation

$$\exp \left\{ \frac{4 \pi^2 M v_0^*}{\alpha h} \right\} \gg 1$$

holds in every case. However, in the expansion for v_f , the relation $v_0^* \gg \sqrt{\frac{2\Delta E}{M}}$ does not hold for any case.

This may well account for the unusually large values of relaxation time predicted.

Schwartz and Herzfeld (29) have extended this work to three dimensions. Most of the corrections occur in the other factors and not in the exponential term. The only correction in this term is brought about by considering

the long range attractive portion of the Lennard-Jones potential. This adds a term $+\frac{\epsilon}{kT}$ to σ above, where ϵ is the height of the potential well. If there is no chemical interaction between the colliding molecules this will be a relatively small term. If chemical interactions take place this can be quite large and give rise to much higher probabilities.

Because of the frequency dependence of this expression, it predicts that for the high frequency vibrational modes the relaxation times will be quite long - in some cases more than a second. Such times can only be qualitatively estimated since one of the assumptions in the derivation is that ΔE is small compared with the translational energies involved. This condition would not be met in the case of high frequency transitions. This would suggest that one line of investigation would be to excite monochromatically the various vibrational modes of a molecule possessing several vibrational frequencies. The relaxation time of each could then be determined while all other parameters than the frequency are held constant. However, Bethe and Teller (3) discussed this problem and concluded that the rate of mixing through anharmonicity of the vibrational modes is much faster than the relaxation process, and that only the lowest frequency relaxation time can be observed. However, their reasoning

is based on a classical model of coupled anharmonic oscillators, whereas in quantum mechanics we expect discrete orthogonal energy states requiring external perturbation for mixing. Even so, with a variety of intermediate states available for stepwise small energy jumps, relaxation to the lowest state can be more efficient than direct decay, and we expect to observe a relaxation time for the lowest frequency only. Measurements made by sound dispersion tend to confirm this. In a great number of observations there has been reported only one case of two relaxation times for a single molecule, that of CH_2Cl_2 by Sette and Hubbard (32). Also, observations have been made by Jacox (19) on a spectrophone apparatus similar to that used in this research to determine the relaxation times of the two active modes of carbon dioxide. She could detect no apparent difference.

Recently there have been correlations made on a large number of measurements on substituted methanes (5, 7, 13, 18, 22, 32) by Fogg, Hanks and Lambert (13), Amme and Legvold (1), and Rossing and Legvold (28). The purpose here was to investigate the dependence of relaxation time on mass and frequency. A plot of $\log Z$ against $\omega^{2/3} M^{1/3}$ was made which showed no regularity for the many measurements. Here $Z = 1/P_{1 \rightarrow 0}$. From this, these workers have concluded that a mechanism based on an energy of

activation gave a better fit with the data. They assumed that the probability could be expressed by

$$P_{1 \rightarrow 0} = \alpha e^{-\frac{\epsilon^*}{kT}} \quad \epsilon^* = nh\nu$$

and found that the data could now be fitted approximately by several straight lines depending on the number of hydrogen atoms in the molecule. The exponential dependence here is given by $c \frac{\omega}{T}$ with no effect of mass.

The evidence to date is far from conclusive. Most investigators have reported a high dependence on reduced collision mass, but no attempt has been made to place this on a quantitative basis. Eucken and Becker (8) found that low molecular weight gases reduced the relaxation time of CO_2 while HCl had an even greater effect on Cl_2 . The latter is probably due to chemical interaction. Smiley and Winkler (35) and McGrath and Ubbelohde (24) reported that their data seemed to fit the exponential $T^{-\frac{1}{3}}$ relation of Schwartz, Slawsky, and Herzfeld, while Eucken and Becker (9, 10, 11, 12) reported an exponential $\{-T^{-1}\}$ dependence. The unusual significance in substituted methanes of the number of hydrogen atoms does not seem to be satisfactorily explained by either theory.

Slobadskaya (34) found that $\text{CO}_2 - \text{CO}_2$ collisions were more efficient in energy exchange than removing excess vibrational energy in CO_2 by air molecules (i.e. principally

CO₂ - N₂ collisions). This would be in opposition to prediction by theory. In contrast, Eucken (7, 8) observed that He, CH₄, and CO were more efficient in relaxing CO₂ molecules than were self collisions, while A and Ne seemed to have roughly the same effect.

EXPERIMENTAL METHODS

The early interest in vibrational relaxation was directed toward velocity of sound measurements and this became the first technique for their estimation (5, 7, 8, 9, 10, 11, 12, 33, 39). The velocity of sound is measured as a function of frequency. The occurrence of dispersion indicates that the transfer of energy into the vibrational modes is no longer keeping up with the fluctuating temperature of the sound wave. The velocity of sound in such a range of sonic frequencies is a known function of the relaxation time, and observation of this dispersion can be used to estimate the rate of energy transfer. This technique still predominates as the most used and many workers are active in this field today (13, 22, 24, 31, 32).

An interesting method is that suggested by Kantrowitz (20) in 1946. In this technique the gas is allowed to expand from a reservoir through a small nozzle. During the expansion, equilibrium is maintained among the various molecular degrees of freedom. The flowing gas then impinges on a pitot tube, and the pressure against the tube is measured. For an equilibrium process the pressure should be that of the reservoir. However, since the impact on the tube is sudden, there is insufficient time for the vibrational modes to come into equilibrium and the pressure

is different from that which would have been expected. The difference in pressure is a function of the relaxation time and can be used in an estimation of this quantity. Measurements have been made on a number of gases by this method. (14, 18).

Stepanov first suggested the use of shock waves for the determination of vibrational relaxation in 1947 (37). A shock front has a very short time duration so that as it passes a region the vibrational degrees of freedom are not in immediate equilibrium. As the shock front passes, equilibrium is gradually established. Using interference techniques, one observes a sudden, sharp fringe shift at the shock front and then the fringes gradually come back to their equilibrium position. The rate of attaining equilibrium is, again, a function of the relaxation process and can be used for an estimation of this time lag. A few measurements have been made employing this technique (15, 35, 36).

The spectrophone was first used for lifetime studies by Slobodskaya in 1948 (34). This device employs a microphone as detector and measures the audiofrequency pulse produced by absorption of infrared light, chopped at the appropriate frequency. There will be a relative phase shift dependent on the life-times of the excited vibrational states from which these lifetimes can be determined.

This latter technique enjoys several advantages over the other techniques. First, it measures directly the rate of loss of energy from vibrational states rather than gain. This makes it possible to maintain the translational temperature at a more nearly constant level than in the other techniques that require an effective surplus of translational over vibrational energy. Also, it enables the study, separately, of the several vibrational modes of more complex molecules. The requirement here, a disadvantage of the method, is that the vibrational mode be infrared active. Further, other methods are limited by the equilibrium amount of energy available to the vibrational degrees, which may be too small to detect in the case of high frequency vibration at room temperature. Use of infrared excitation raises the vibrational energy to a sufficiently high level. This last technique will be employed in the study of carbon monoxide in mixtures with various gases.

ELEMENTARY SPECTROPHONE PROCESSES

It is essential in order to evaluate the data obtained in the spectrophone method, to have some understanding of the energy relations occurring within the cell. In completing the analysis some simplifying assumptions will be made that should permit order of magnitude estimations of the various effects. Turrell (38) has considered the problem from the point of view of generation of a sound wave which is dissipated while traveling in the cell. This view may well be correct in the case of CO_2 in which all of the radiation is virtually absorbed at the optical entrance of the cell and must be distributed throughout the cell by means of wave propagation. However, for CO , which is a much weaker absorber than CO_2 , the radiant energy is more evenly distributed throughout the cell. This would result in a more uniform pressure and not give rise to sound waves. Such a system would be better considered as a problem in heat transfer, and it is the purpose of this section to complete such an analysis.

We can assume that the rate of absorption throughout the cell is proportional to the intensity and obeys Beer's law. Thus the rate of increase of vibrational energy, E_v , by absorption is $\mathcal{K}I$. This energy is removed by the relaxation process which, according to Schwartz,

Slawsky, and Herzfeld (30), can be written $\frac{1}{\tau} [E_v - E(T)]$. $E(T)$ is the Einstein function expressing the equilibrium amount of vibrational energy at the translational temperature T . τ , then, is the vibrational relaxation time. This gives

$$\frac{dE_v}{dt} = \kappa I - \frac{1}{\tau} [E_v - E(T)]$$

We are interested in the increase in translational temperature $\Theta = T - T_0$ where T_0 is the temperature of the surroundings to which the energy is being dissipated. Then, if c_v is the heat capacity of the vibrational degrees of freedom at T_0 , to a very good first approximation we can write $E(T) = E(T_0) + c_v \Theta$.

Assuming a periodic light source, it can be represented by $I = \frac{I_0}{2} (1 + \sin \omega t) f(x, r, \phi)$ where $f(x, r, \phi)$ is the intensity distribution spatially throughout the cylindrical cell. From Beer's law the x behavior is expressed as $e^{-\kappa x}$ and we can assume the light has angular symmetry, i.e., is not a function of ϕ . Further, since the light beam essentially fills the cell, we can assume that the radial dependence is constant. Then I is given by

$$I = \frac{I_0}{2} (1 + \sin \omega t) e^{-\kappa x}$$

throughout the cell. This gives

$$\frac{dE_v}{dt} = \frac{\kappa I_0}{2} (1 + \sin \omega t) e^{-\kappa x} - \frac{1}{\tau} [E_v - E_0(T_0) - c_v \theta] \quad (1)$$

Translational energy is increased by the relaxation process and decreased by heat flow. This can be formulated by

$$c \frac{d\theta}{dt} = k \nabla^2 \theta + \frac{1}{\tau} [E_v - E_0 - c_v \theta] \quad (2)$$

From (1) and (2) we can derive an equation not explicitly involving E_v that can be solved for θ . Since the pressure fluctuations within the cell are a function of θ , the behavior of this quantity will describe the response of the microphone.

From (2), then, we have

$$E_v = c \tau \frac{d\theta}{dt} - \tau k \nabla^2 \theta + E_0 + c_v \theta$$

$$\text{and } \frac{dE_v}{dt} = c \tau \frac{d^2\theta}{dt^2} - \tau k \nabla^2 \frac{d\theta}{dt} + c_v \frac{d\theta}{dt}$$

Combining with (1) we obtain

$$c \tau \frac{d^2\theta}{dt^2} - \tau k \nabla^2 \frac{d\theta}{dt} + c_v \frac{d\theta}{dt} =$$

$$\frac{\kappa I_0}{2} (1 + \sin \omega t) e^{-\kappa x} - c \frac{d\theta}{dt} + k \nabla^2 \theta - \frac{1}{\tau} E_0 -$$

$$\frac{c_v}{\tau} \theta + \frac{1}{\tau} E_0 + \frac{c_v}{\tau} \theta$$

$$c\tau \frac{d^2\theta}{dt^2} - k\nabla^2\left(\theta + \tau \frac{d\theta}{dt}\right) + (c + c_v) \frac{d\theta}{dt} = \frac{\kappa I_0}{2} (1 + \sin \omega t) e^{-\kappa x} \quad (3)$$

We are interested here, not in transients, but in a steady state solution, so that we may assume for time dependence the imposed functions $\sin \omega t$ and $\cos \omega t$. θ , then, can be expressed as

$$\begin{aligned} \theta &= U_0(x, r, \phi) + U_1(x, r, \phi) \sin \omega t + U_2(x, r, \phi) \\ &\qquad \qquad \qquad \cos \omega t \qquad \qquad \qquad (4) \\ &= U_0(x, r, \phi) + U(x, r, \phi) \sin(\omega t + \beta) \end{aligned}$$

The cell itself is a cylinder with a steel wall at $r = a$, and rock salt windows at $x = 0$ and $x = L$. The boundary materials have much higher heat conductivities than the gas itself, so it can be assumed that at each of these boundaries, $\theta = 0$. This can only be satisfied if U_0 , U_1 , and U_2 are each in turn zero at the boundaries. The microphone is situated effectively at the cell wall, centered lengthwise, where it is assumed that $\theta = 0$. However, we observe that no matter what the distribution of θ at any given instant, the pressure change must remain fairly constant throughout the cell and be proportional to the average value of θ throughout the cell volume. Thus,

in order to get the pressure dependence, the solution for Θ will be averaged over the volume of the cell.

An exact solution of (3) is difficult and may not lead to a physically meaningful solution. Using the method of separation of variables we assume solutions of the form

$$U_i = X_i(x) \cdot R_i(r)$$

The angular symmetry of the radiation suggests a similar symmetry in the solution. We do not know the exact solutions for X_i and R_i but we do know that whatever their form, they can be expanded in terms of a Fourier series and in terms of zeroth order Bessel functions, respectively, which satisfy the boundary conditions.

$$X_i = \sum_{n=1}^{\infty} A_n^i \sin \frac{n\pi}{L} x$$

$$R_i = \sum_{m=1}^{\infty} B_m^i J_0\left(\frac{\lambda_m}{a} r\right)$$

$$\lambda_m = m^{\text{th}} \text{ zero of } J_0(z)$$

Better yet, this can be written

$$U_i = \sum_{n=1}^{\infty} \sum_{m=1}^{\infty} A_{n,m}^i \sin \frac{n\pi}{L} x J_0\left(\frac{\lambda_m}{a} r\right) \quad (6)$$

The constants $A_{n,m}^i$ can be found by substitution into equation (3), observing that $\frac{\kappa I_0}{2} e^{-\kappa x}$ can also be expanded:

$$\frac{\kappa I_0}{2} e^{-\kappa x} = \sum_{n=1}^{\infty} \sum_{m=1}^{\infty} C_{n,m} \sin \frac{n\pi x}{L} J_0\left(\frac{\lambda_m}{a} r\right) \quad (7)$$

This expansion will give the proper value at every interior point of the cell, and will be zero on the boundaries (as, indeed, it should).

Substituting (4) into (3) we have

$$\theta = U_1 \sin \omega t + U_2 \cos \omega t + U_0$$

$$\frac{d\theta}{dt} = U_1 \omega \cos \omega t - U_2 \omega \sin \omega t$$

$$\frac{d^2\theta}{dt^2} = -U_1 \omega^2 \sin \omega t - U_2 \omega^2 \cos \omega t, \quad \text{which}$$

leads to

$$\begin{aligned} & -c\tau\omega^2 U_1 \sin \omega t - c\tau\omega^2 U_2 \cos \omega t \\ & -(c + c_v) \omega U_1 \cos \omega t - (c + c_v) \omega U_2 \sin \omega t \\ & -k\tau\omega \nabla^2 U_1 \cos \omega t + k\tau\omega \nabla^2 U_2 \sin \omega t \\ & -k \nabla^2 U_1 \sin \omega t - k \nabla^2 U_2 \cos \omega t - k \nabla^2 U_0 \\ & = \frac{\kappa I_0}{2} (1 + \sin \omega t) e^{-\kappa x}, \end{aligned}$$

which gives

$$-k \nabla^2 U_0 = \frac{\kappa I_0}{2} e^{-\kappa x} \quad (8)$$

$$-c\tau\omega^2 U_1 - \omega(c + c_v) U_2 + k\tau\omega \nabla^2 U_2 -$$

$$k \nabla^2 U_1 = \frac{\kappa I_0}{2} e^{-\kappa x} \quad (9)$$

$$-c\tau\omega^2 U_2 + \omega(c + c_v)U_1 - k\tau\omega\nabla^2 U_1 - k\nabla^2 U_2 = 0 \quad (10)$$

From (8), (7), and (6)

$$\begin{aligned} & -k \sum_{n=1}^{\infty} \sum_{m=1}^{\infty} A_{n,m}^0 \nabla^2 \sin \frac{n\pi x}{L} J_0\left(\frac{\lambda_m r}{a}\right) \\ & = \sum_{n=1}^{\infty} \sum_{m=1}^{\infty} C_{n,m} \sin \frac{n\pi x}{L} J_0\left(\frac{\lambda_m r}{a}\right) \\ & kA_{n,m}^0 \left(\frac{n^2 \pi^2}{L^2} + \frac{\lambda_m^2}{a^2} \right) = C_{n,m} \\ & A_{n,m}^0 = \frac{C_{n,m}}{k \left(\frac{n^2 \pi^2}{L^2} + \frac{\lambda_m^2}{a^2} \right)} \\ & C_{n,m} = \frac{\kappa I_0}{2} \frac{2}{L} \frac{2}{a^2 J_1(\lambda_m)} \int_0^L e^{-\kappa x} \sin \frac{n\pi x}{L} dx \\ & \quad \int_0^a r J_0\left(\frac{\lambda_m r}{a}\right) dr \\ & = 2 \kappa I \frac{n\pi}{L} \frac{1}{\lambda_m J_1(\lambda_m)} \frac{1 - e^{-\kappa L} (-1)^n}{\kappa + \frac{n^2 \pi^2}{L^2}} \end{aligned}$$

We are more particularly interested in the oscillating part of the solution given by U_1 and U_2 , which can be found from equations (9) and (10). Substituting equations (6) and (7) into (9) and (10) gives

$$\begin{aligned} & -c\tau\omega^2 \sum_{n=1}^{\infty} \sum_{m=1}^{\infty} A_{n,m}^1 \sin \frac{n\pi x}{L} J_0\left(\frac{\lambda_m r}{a}\right) \\ & - \omega(c + c_v) \sum_{n=1}^{\infty} \sum_{m=1}^{\infty} A_{n,m}^2 \sin \frac{n\pi x}{L} J_0\left(\frac{\lambda_m r}{a}\right) \end{aligned}$$

$$\begin{aligned}
& + k \tau \omega \sum_{n=1}^{\infty} \sum_{m=1}^{\infty} \left(-\frac{n^2 \pi^2}{L^2} - \frac{\lambda_m^2}{a^2} \right) A_{n,m}^2 \sin \frac{n\pi x}{L} J_0 \left(\frac{\lambda_m r}{a} \right) \\
& - k \sum_{n=1}^{\infty} \sum_{m=1}^{\infty} \left(-\frac{n^2 \pi^2}{L^2} - \frac{\lambda_m^2}{a^2} \right) A_{n,m}^1 \sin \frac{n\pi x}{L} J_0 \left(\frac{\lambda_m r}{a} \right) \\
& = \sum_{n=1}^{\infty} \sum_{m=1}^{\infty} C_{n,m} \sin \frac{n\pi x}{L} J_0 \left(\frac{\lambda_m r}{a} \right) \quad (11)
\end{aligned}$$

$$\begin{aligned}
\text{and } & - c \tau \omega^2 \sum_{n=1}^{\infty} \sum_{m=1}^{\infty} A_{n,m}^2 \sin \frac{n\pi x}{L} J_0 \left(\frac{\lambda_m r}{a} \right) \\
& + \omega (c + c_v) \sum_{n=1}^{\infty} \sum_{m=1}^{\infty} A_{n,m}^1 \sin \frac{n\pi x}{L} J_0 \left(\frac{\lambda_m r}{a} \right) \\
& - k \tau \omega \sum_{n=1}^{\infty} \sum_{m=1}^{\infty} \left(-\frac{n^2 \pi^2}{L^2} - \frac{\lambda_m^2}{a^2} \right) A_{n,m}^1 \sin \frac{n\pi x}{L} J_0 \left(\frac{\lambda_m r}{a} \right) \\
& - k \sum_{n=1}^{\infty} \sum_{m=1}^{\infty} \left(-\frac{n^2 \pi^2}{L^2} - \frac{\lambda_m^2}{a^2} \right) A_{n,m}^2 \sin \frac{n\pi x}{L} J_0 \left(\frac{\lambda_m r}{a} \right) \quad (12)
\end{aligned}$$

(11) and (12) give rise to the infinite set of simultaneous equations

$$\begin{aligned}
& \left[k \left(\frac{n^2 \pi^2}{L^2} + \frac{\lambda_m^2}{a^2} \right) - c \omega^2 \tau \right] A_{n,m}^1 - \omega \left[c + c_v \right. \\
& \left. + k \tau \left(\frac{n^2 \pi^2}{L^2} + \frac{\lambda_m^2}{a^2} \right) \right] A_{n,m}^2 = C_{n,m} \quad (13)
\end{aligned}$$

$$\begin{aligned}
\text{and } & \omega \left[c + c_v + k \tau \left(\frac{n^2 \pi^2}{L^2} + \frac{\lambda_m^2}{a^2} \right) \right] A_{n,m}^1 + \left[k \left(\frac{n^2 \pi^2}{L^2} + \frac{\lambda_m^2}{a^2} \right) - \right. \\
& \left. c \omega^2 \tau \right] A_{n,m}^2 = 0 \quad (14)
\end{aligned}$$

$$\text{Let } \alpha = c \omega^2 \tau - k \left(\frac{n^2 \pi^2}{L^2} + \frac{\lambda_m^2}{a^2} \right) \quad (15)$$

$$\text{and } \mathcal{J} = \omega \left[c + c_v + k\tau \left(\frac{n^2 \pi^2}{L^2} + \frac{\lambda_m^2}{a^2} \right) \right] \quad (16)$$

(13) and (14) become

$$-\alpha A_{n,m}^1 - \mathcal{J} A_{n,m}^2 = C_{n,m}$$

$$\text{and } \mathcal{J} A_{n,m}^1 - \alpha A_{n,m}^2 = 0$$

the solutions of which are

$$A_{n,m}^1 = - \frac{\alpha}{\alpha^2 + \mathcal{J}^2} C_{n,m}$$

$$\text{and } A_{n,m}^2 = - \frac{\mathcal{J}}{\alpha^2 + \mathcal{J}^2} C_{n,m}$$

The solution for θ now becomes

$$\theta = \sum_{n=1}^{\infty} \sum_{m=1}^{\infty} \left\{ \frac{1}{k \left(\frac{n^2 \pi^2}{L^2} + \frac{\lambda_m^2}{a^2} \right)} - \frac{\alpha}{\alpha^2 + \mathcal{J}^2} \sin \omega t - \frac{\mathcal{J}}{\alpha^2 + \mathcal{J}^2} \cos \omega t \right\} \left\{ C_{n,m} \sin \frac{n\pi x}{L} J_0 \left(\frac{\lambda_m r}{a} \right) \right\} \quad (17)$$

and for the phase shift

$$\tan \beta = \frac{\sum_{n=1}^{\infty} \sum_{m=1}^{\infty} \frac{\mathcal{J}}{\alpha^2 + \mathcal{J}^2} C_{n,m} \sin \frac{n\pi x}{L} J_0 \left(\frac{\lambda_m r}{a} \right)}{\sum_{n=1}^{\infty} \sum_{m=1}^{\infty} \frac{\alpha}{\alpha^2 + \mathcal{J}^2} C_{n,m} \sin \frac{n\pi x}{L} J_0 \left(\frac{\lambda_m r}{a} \right)} \quad (18)$$

where α and \mathcal{J} are given by (15) and (16) while $C_{n,m}$ has been evaluated previously.

This solution is to be averaged over the volume of the

cell. It is easily demonstrated that

$$\begin{aligned} \frac{1}{V} \int_0^{2\pi} \int_0^a \int_0^L C_{n,m} \sin \frac{n\pi x}{L} J_0 \left(\frac{\lambda_m r}{a} \right) r dx dr d\theta \\ = 8 \kappa I_0 \frac{1 + e^{-\kappa L}}{L} \frac{1}{\kappa^2 + \frac{n^2 \pi^2}{L^2}} \frac{1}{\lambda_m^2} \quad (n \text{ odd}) \end{aligned}$$

which gives

$$\begin{aligned} \bar{\Theta} = \bar{\Theta}_0 - \sum_{n=1}^{\infty} \sum_{m=1}^{\infty} \left\{ \alpha \sin \omega t + \delta \cos \omega t \right\} \\ \left\{ \frac{8\kappa I_0 (1 + e^{-\kappa L})}{L (\alpha^2 + \delta^2)} \frac{1}{\kappa^2 + \frac{n^2 \pi^2}{L^2}} \frac{1}{\lambda_m^2} \right\} \end{aligned} \quad (19)$$

Here the details of the steady state solution are neglected, since it is only the periodic part that will give phase shift information. Assuming that $\kappa < \frac{\pi}{L}$ (see Appendix II) and combining the sine and cosine terms we have

$$\begin{aligned} \bar{\Theta} = \bar{\Theta}_0 - \frac{8\kappa I_0 (1 + e^{-\kappa L}) L}{\pi^2} \sum_{n=1}^{\infty} \sum_{m=1}^{\infty} B_{n,m} \\ \sin(\omega t + \phi_{n,m}); \quad B_{n,m} = \frac{1}{n^2} \frac{1}{\lambda_m^2} \frac{1}{(\alpha^2 + \delta^2)^{\frac{1}{2}}}; \end{aligned}$$

$$\tan \phi_{n,m} = \frac{\delta}{\alpha} \quad (20)$$

$$\text{Let } \gamma_{m,n} = \left(\frac{n^2 \pi^2}{L^2} + \frac{\lambda_m^2}{a^2} \right) \frac{k}{c\omega}$$

$$\begin{aligned} \alpha^2 + \delta^2 = c^2 \omega^4 \tau^2 + \gamma_{m,n}^2 c^2 \omega^2 - 2c^2 \omega^3 \tau \gamma_{m,n} \\ + (c + c_v)^2 \omega^2 + c^2 \omega^4 \tau^2 \gamma_{m,n}^2 \end{aligned}$$

$$+ 2(c + c_v)c\omega^3\tau \delta_{m,n}$$

Since for carbon monoxide $c_v \ll c$, we can write

$$\alpha^2 + \delta^2 = (1 + \omega^2\tau^2) (1 + \delta_{m,n}^2)c^2\omega^2$$

$$\tan \phi_{n,m} = \frac{\omega c + \omega\tau\omega c \delta_{m,n}}{\omega c \omega\tau - \omega c \delta_{m,n}} = \frac{1}{\omega\tau} + \frac{\delta_{m,n}}{1 - \frac{1}{\omega\tau} \delta_{m,n}}$$

$$\text{Let } \tan \phi_0 = \frac{1}{\omega\tau} \quad \tan \phi'_{n,m} = \delta_{m,n}$$

Then we can see that $\phi_{n,m} = \phi_0 + \phi'_{n,m}$ and equation (20) becomes

$$\begin{aligned} \bar{\theta} &= \bar{\theta}_0 - \frac{8\kappa I_0(1 + e^{-\kappa L})L}{\pi^2 c \omega (1 + \omega^2\tau^2)^{\frac{1}{2}}} \\ &= \bar{\theta}_0 - G \sum_{\substack{n=1 \\ \text{odd}}}^{\infty} \sum_{m=1}^{\infty} \left\{ B'_{n,m} \sin(\omega\tau + \phi_0 + \phi'_{n,m}) \right\} \\ &= \bar{\theta}_0 - G \sum_{\substack{n=1 \\ \text{odd}}}^{\infty} \sum_{m=1}^{\infty} \left\{ B'_{n,m} \cos \phi'_{n,m} \sin(\omega\tau + \phi_0) + \right. \\ &\quad \left. B'_{n,m} \sin \phi'_{n,m} \cos(\omega\tau + \phi_0) \right\} \\ &= \bar{\theta}_0 - G \sin(\omega\tau + \phi_0) \sum_{\substack{n=1 \\ \text{odd}}}^{\infty} \sum_{m=1}^{\infty} B'_{n,m} \cos \phi'_{n,m} - \\ &\quad G \cos(\omega\tau + \phi_0) \sum_{\substack{n=1 \\ \text{odd}}}^{\infty} \sum_{m=1}^{\infty} B'_{n,m} \sin \phi'_{n,m} \quad (21) \end{aligned}$$

$$\text{where } B'_{n,m} = \frac{1}{n^2} \frac{1}{\lambda_m^2} \frac{1}{(1 + \delta_{m,n}^2)^{\frac{1}{2}}};$$

$$G = \frac{8\kappa I_0(1 + e^{-\kappa L})L}{\pi^2 c \omega (1 + \omega^2\tau^2)^{\frac{1}{2}}}$$

$$\sin \phi'_{n,m} = \frac{\gamma_{m,n}}{(1 + \gamma_{m,n}^2)^{\frac{1}{2}}} ; \cos \phi'_{n,m} = \frac{1}{(1 + \gamma_{m,n}^2)^{\frac{1}{2}}}$$

The solution is now seen to have the form

$$\bar{\theta} = \bar{\theta}_0 - G' \sin(\omega\tau + \phi_0 + \bar{\phi})$$

where $\phi_0 = \tan^{-1} \frac{1}{\omega\tau}$ is the phase shift due to relaxation and

$$\bar{\phi} = \tan^{-1} \frac{\sum_{n=1}^{\infty} \sum_{m=1}^{\infty} \frac{1}{n^2} \frac{1}{\lambda_m^2} \frac{\gamma_{m,n}}{1 + \gamma_{m,n}^2}}{\sum_{n=1}^{\infty} \sum_{m=1}^{\infty} \frac{1}{n^2} \frac{1}{\lambda_m^2} \frac{1}{1 + \gamma_{m,n}^2}} \quad (n \text{ odd})$$

is the phase shift due to heat conduction effects.

In Appendix II an approximate solution for $\bar{\phi}$ is obtained by evaluating the sums in numerator and denominator under the assumption that $\gamma_{m,n}$ is only appreciable for large values of m and n and is a very slowly varying function of these integers. The result is

$$\tan \bar{\phi} = \left(\frac{2k}{\omega c}\right) \left(\frac{1}{L} + \frac{1}{a}\right) \quad (22)$$

The total phase shift can now be seen to be

$$\begin{aligned} \phi &= \phi_0 + \bar{\phi} = \tan^{-1} \frac{\frac{1}{\omega\tau} + \left(\frac{2k}{\omega c}\right)^{\frac{1}{2}} \left(\frac{1}{L} + \frac{1}{a}\right)}{1 - \frac{1}{\omega\tau} \left(\frac{2k}{\omega c}\right)^{\frac{1}{2}} \left(\frac{1}{L} + \frac{1}{a}\right)} \\ &= \tan^{-1} \frac{1 + \omega\tau \left(\frac{2k}{\omega c}\right)^{\frac{1}{2}} \left(\frac{1}{L} + \frac{1}{a}\right)}{\omega\tau - \left(\frac{2k}{\omega c}\right)^{\frac{1}{2}} \left(\frac{1}{L} + \frac{1}{a}\right)} \quad (23) \end{aligned}$$

Here we have assumed that $\left(\frac{2k}{\omega c}\right)^{\frac{1}{2}} \left(\frac{1}{L} + \frac{1}{a}\right) \ll 1$ and we will

further assume that $\omega\tau < 1$. We can then make the

approximation $\phi = \tan^{-1} \frac{1}{\omega\tau - \left(\frac{2k}{\omega c}\right)^{\frac{1}{2}} \left(\frac{1}{L} + \frac{1}{a}\right)}$ (24)

If $\omega\tau \left(\frac{2k}{\omega c}\right)^{\frac{1}{2}} \left(\frac{1}{L} + \frac{1}{a}\right) \gg 1$ we can see that the phase shift becomes

$$\tan^{-1} \left(\frac{2k}{\omega c}\right)^{\frac{1}{2}} \left(\frac{1}{L} + \frac{1}{a}\right) \text{ and is independent of } \tau .$$

However, such relaxation times seem very unlikely, and, indeed, have not been observed in this research.

In order for the phase shift to be primarily dependent on the relaxation time we must have

$$\left(\frac{2k}{\omega c}\right)^{\frac{1}{2}} \left(\frac{1}{L} + \frac{1}{a}\right) \text{ which places a lower limit on the}$$

observable τ 's. Evaluation of these quantities in Appendix II demonstrates that the inequality holds at least for this experiment.

It appears in expression (24) that the range of measurable relaxation times can be increased simply by increasing the value of ω , the chopping frequency. This is limited, however, by the desirability of keeping $\omega\tau$ small, i.e. less than unity. It would be desirable, then, to be able to vary ω over a range of frequencies, so that for the range of relaxation times being studied the inequalities $1 > \omega\tau > \left(\frac{2k}{\omega c}\right)^{\frac{1}{2}} \left(\frac{1}{L} + \frac{1}{a}\right)$ are

are satisfied.

If $\omega\tau \gg 1$ we can expand $\tan \phi_0 = \frac{1}{\omega\tau}$ to obtain the phase shift in terms of the relaxation time, τ , in a linear approximation.

$$\phi_0 = \tan^{-1} \frac{1}{\omega\tau} \approx \frac{\pi}{2} - \omega\tau \dots\dots\dots$$

The values of $\omega\tau$ for which this approximation holds are discussed in Appendix III.

Hidden in the above discussion is the significance of the term κ , the integrated absorption coefficient, in its effect on the phase shift. This can be more satisfactorily discussed if the problem is restated, knowing that the solution has approximately the form

$$U_1 = Ae^{-\kappa x} \quad U_2 = Be^{-\kappa x} \quad (25)$$

Substitution into (9) and (10) gives

$$-c\tau\omega^2 A - \omega(c + c_v)B + k\omega\tau\kappa^2 B - k\kappa^2 A = \frac{\kappa I_0}{2}$$

$$-c\tau\omega^2 B + \omega(c + c_v)A - k\omega\tau\kappa^2 A - k\kappa^2 B = 0$$

$$-\alpha A - \delta B = \frac{\kappa I_0}{2} \quad \delta A - \alpha B = 0$$

$$\alpha = c\omega^2\tau + k\kappa^2 \quad \delta = \omega(c + c_v - k\tau\kappa^2)$$

$$A = -\frac{\alpha}{\alpha^2 + \delta^2} \frac{\kappa I_0}{2} \quad B = -\frac{\delta}{\alpha^2 + \delta^2} \frac{\kappa I_0}{2}$$

$$\tan \beta = \frac{B}{A} = \frac{d}{\alpha} = \frac{\omega (c + c_v - k\tau \kappa^2)}{c\omega^2\tau + k\kappa^2} \quad (26)$$

From this expression we can see that in order for the phase shift to be given by $\tan \beta = \frac{1}{\omega\tau}$ we must have

$\omega\tau \gg \frac{k\kappa^2}{\omega c}$. In Appendix II this inequality is demon-

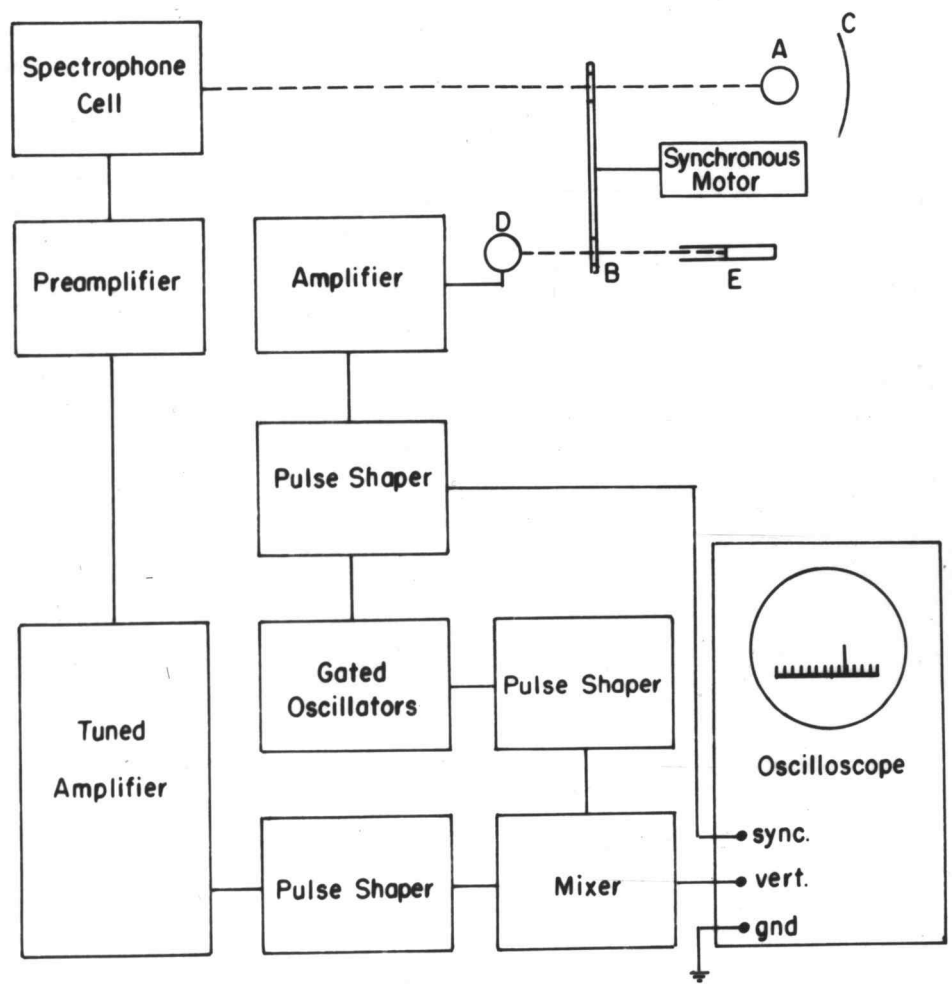
strated for carbon monoxide. However, care must be taken to insure that this relation is satisfied before meaningful phase shifts can be measured. For sufficiently large values of κ (i.e. CO₂) and small values of ω this relation can break down so that the phase shift observed is that due to energy distribution rather than relaxation processes. This may account for the high apparent efficiency of carbon dioxide in self-collisions observed by Slobadskaya (34).

EXPERIMENTAL TECHNIQUE

The equipment used in this research is essentially that designed and described by George Turrell (38), the only modification being redesign of the preamplifier to give a better signal to noise ratio. A block diagram of this apparatus is given in Figure I. The light source (A) consists of a carbon arc mounted in an arc projector chassis. One of the principal experimental difficulties encountered was due to instabilities in the burning of this arc. To surmount this problem, great care was taken to adjust the carbon rods to nearly the same position for each reading and in no case was a reading taken on a fresh carbon rod until it had burned down to a fairly constant shape. Further, for each point obtained at least ten readings were taken in rapid succession to get a good average value for the position of the marker.

The light from (A) was focused by mirror (B) onto a plexiglas chopper (C) and then into the spectrophone cell. The chopper was driven by a synchronous motor with an angular frequency of 1800 revolutions per minute. Since the plexiglas chopper contains twenty orifices around its face, this gives a light chopping frequency of 600 cycles per second. The synchronous motor itself can serve as a fair timing standard. To obtain a stable reference signal,

Fig.I
BLOCK DIAGRAM OF SPECTROPHONE



a phototube (D) was so placed as to receive light from a small directional light source (E) through the plexiglas chopper at a radius inside that at which the holes are located. A small piece of black tape on the plexiglas interrupts this light source once every thirtieth of a second to send a pulse through the phototube assembly and trigger the oscilloscope sweep as well as the gated oscillator.

The time base was given by a gated oscillator designed to give markers every 10^{-4} seconds. The separation of two spectrophone signals is determined by the synchronous motor and, hence, can be used to calibrate the time base. This separation is $1/600$ of a second or 16.7×10^{-4} seconds. That is, two successive spectrophone signals should lie 16.7 time base markers apart. In actual observation this was found to be about 16.5 ± 0.3 , amounting to about a 2% error in the time base.

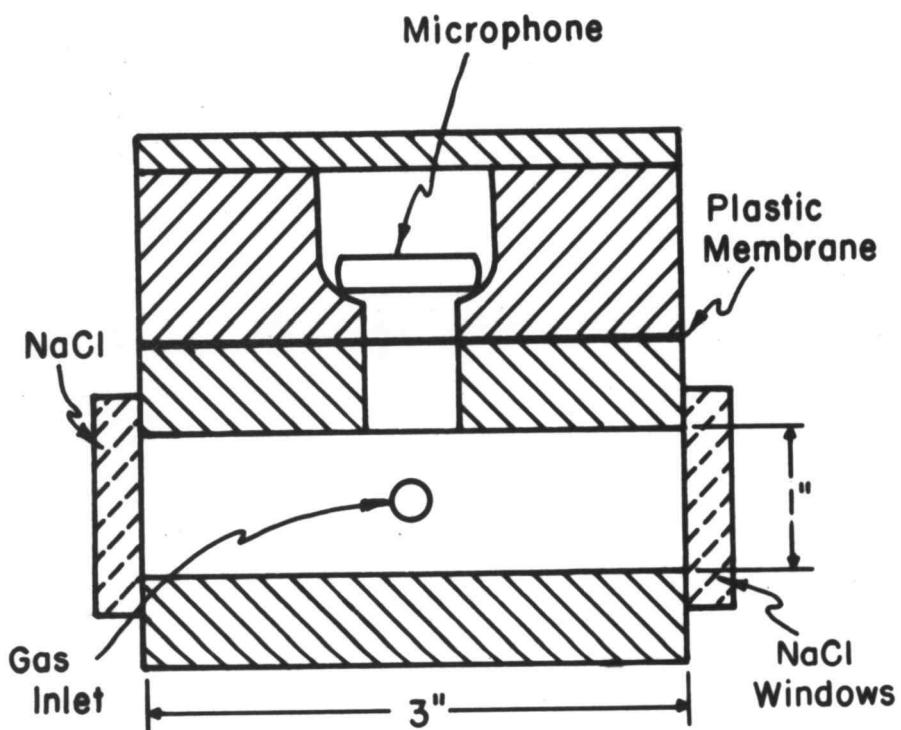
For this research no light filter was employed since carbon monoxide has only one fundamental absorption in the infrared region and, hence, only this one type of relaxation can contribute to the observed phase shifts. However, since a light continuum was used, care had to be exercised to select infrared inert diluents for study as well as to preclude any but the barest trace of impurities that absorb very strongly in the infrared. It was found

that samples unusually rich in CO_2 or not purified through a cold trap gave significant deviation from comparable samples without appreciable CO_2 or water vapor.

The spectrophone cell itself was prepared from a block of steel. A cross sectional diagram can be seen in Figure II. Infrared light passes through the NaCl windows from left to right. An outlet on the side for sampling purposes can be seen in the center. At the top of this chamber an access is permitted to the microphone chamber through the coupling of a plastic (Saranwrap) membrane. This permitted evacuation of the cell without damage to the microphone as well as permitting a constant (atmospheric pressure) loading of the microphone diaphragm. The microphone itself is a rochelle salt crystal microphone of a design for use in hearing aid systems. The interior of the gas filled portion of the cell is one inch in diameter and three inches long.

The technique employed is that used by Turrell, in which measurements are taken alternately on the mixture being analysed and then on tank carbon monoxide used as a standard. The major deviation in method here was to repeat the measurements on any given mixture several times to give a good average value. In this way data was taken on mixtures of carbon monoxide with hydrogen, helium, neon, and argon.

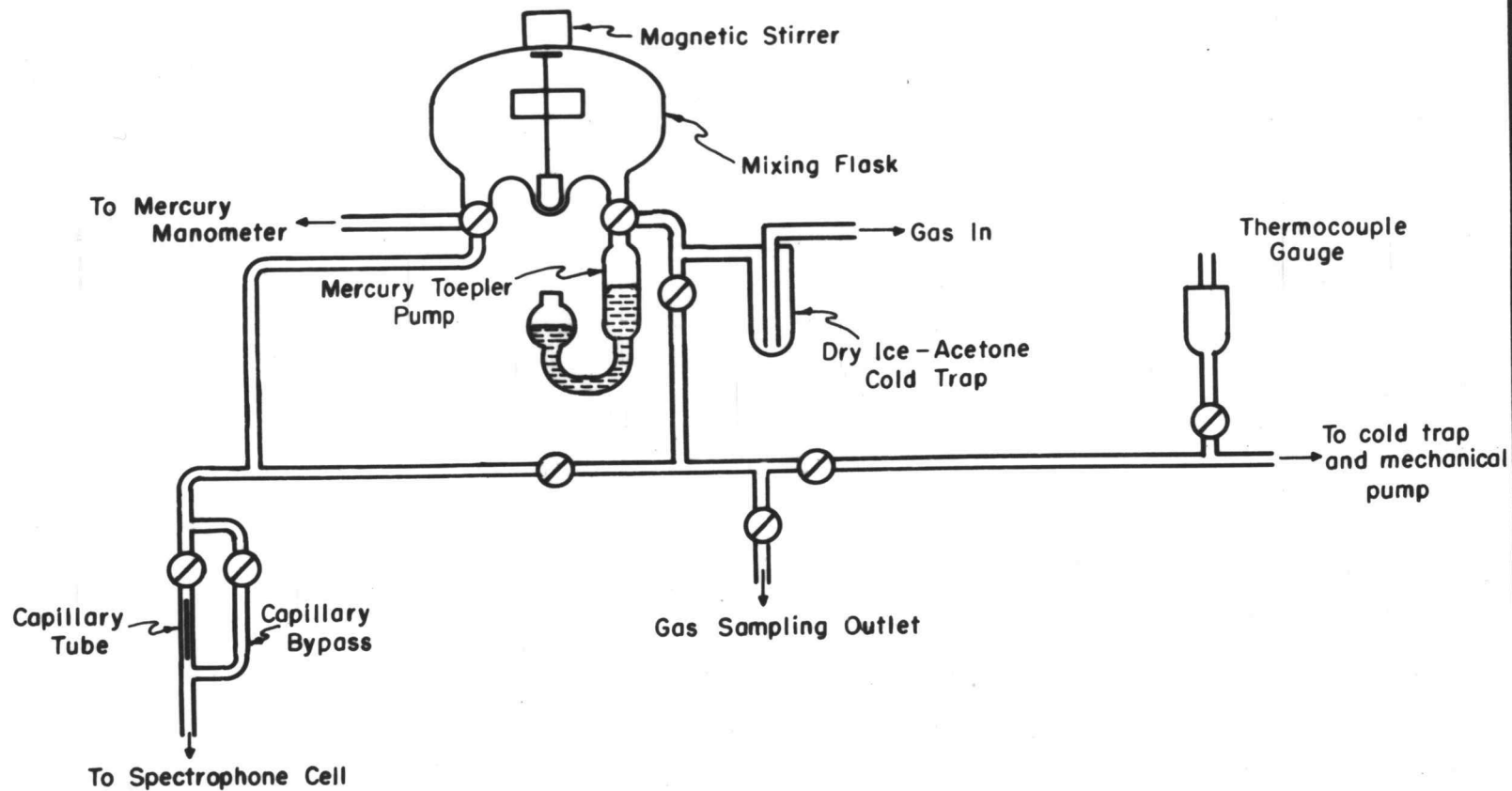
Fig. II
SPECTROPHONE CELL



A possible criticism of Turrell's work is that he did not take sufficient precaution to insure proper mixing of gases introduced into his cell. To insure complete mixing in this research, a portable gas handling system was constructed with a three liter chamber for preparing gas mixtures. The gases were introduced into this chamber and agitated for at least ten minutes before being introduced into the spectrophone cell for analysis. Agitation was accomplished by means of a magnetically coupled stirrer encased in the mixing flask. The gases were passed through a dry ice acetone cold trap before entering the flask to remove any water vapor and traces of higher boiling organic compounds. Figure III gives a schematic diagram of the gas handling system while Figure IV is a picture of this apparatus. Samples for mass spectrometric analysis were taken of various gases through the gas sampling outlet, and flasks of reagent grade neon and carbon monoxide were introduced through this outlet. A sample of tank carbon monoxide was treated in this manner and then analysed on the mass spectrometer. No appreciable contamination of the sample with low molecular weight (below mass 30) vapors, such as hydrocarbons, could be detected.

Mixtures were carefully prepared by introducing tank carbon monoxide into the flask to a pressure measured by the mercury manometer, after first evacuating the flask to

Fig. III
Schematic Diagram of Gas Handling Apparatus



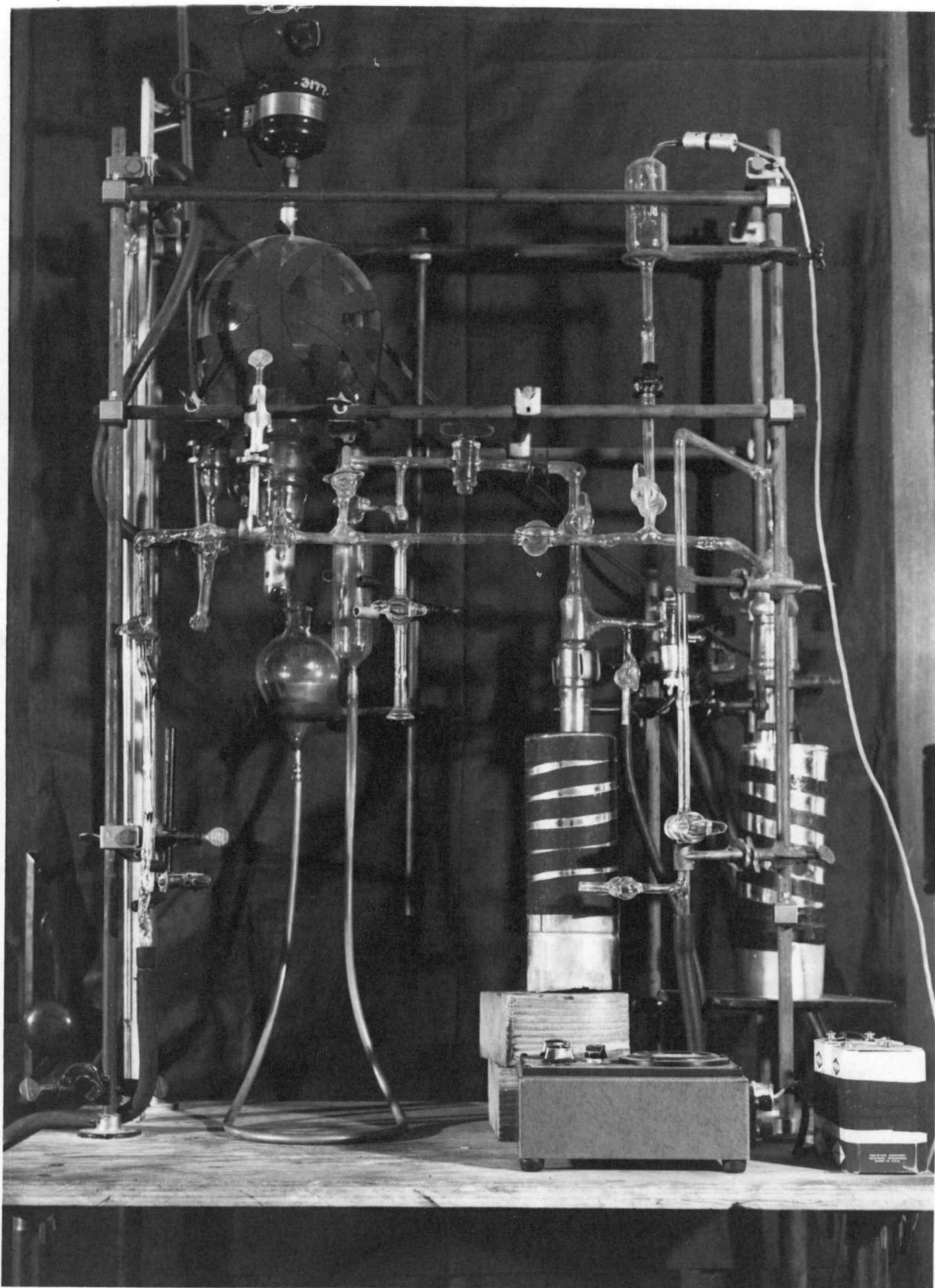


FIGURE IV
GAS HANDLING SYSTEM

a pressure of 10^{-2} cm of mercury as measured by the thermocouple gauge. The flask was then sealed off from the manometer and the diluting gas was pipetted in by means of the Toepler pump. It was first necessary to calibrate the ratio of pipette to mixing flask and to calibrate the thermocouple gauge. The thermocouple gauge was calibrated by means of a McLeod gauge designed for pressures of 10 to 1000 microns of mercury. The pipette was calibrated by evacuating the mixing flask and admitting ten pipettes of gas at one atmosphere pressure and observing the resultant pressure within the flask by means of the mercury manometer. The volume of the flask was corrected for the slight additional volume of the manometer.

After the mixture had been agitated for ten minutes it was introduced into the spectrophone cell at slightly above one atmosphere by means of the Toepler pump. The cell was then opened to the atmosphere to equalize the pressure and a measurement taken. The cell was then immediately evacuated and filled with carbon monoxide directly from the tank, and in a similar way a measurement was made on the tank carbon monoxide. The difference between these two measurements is the Δt to be used in the analysis described in Appendix IV. This cycle was repeated several times to obtain a good average value.

Since all commercially available carbon monoxide

contains up to a few per cent hydrogen, and theory predicts that the relaxation time is very sensitive to low molecular weight gases such as hydrogen, it was considered essential first to establish the relaxation time for hydrogen-carbon monoxide collisions, and, concomitantly, to establish the relaxation time of tank carbon monoxide as well as that due to carbon monoxide in self collisions. The procedure followed here is outlined in Appendix IV.

This completed, it was then possible to use tank carbon monoxide as an absolute standard in measurements on other gas mixtures, which necessitates a fewer number of determinations for each relaxing gas.

Mass spectrometric analysis was used to determine the exact amount of hydrogen impurity available in the commercial carbon monoxide as well as to look for traces of low molecular weight compounds. Samples for analysis were processed through the gas handling system in the same way as for spectrophone measurements and then collected in a tube fitted with stopcock and taper joint to fit the mass spectrometer. Studies on early mixtures were carried out on the instrument constructed at the University of Oregon under the direction of Dr. D. F. Swineheart. This machine employs a mercury diffusion pump and liquid air traps. This keeps the background for low molecular weight components other than mass numbers

14, 16, 17, 18, 28, 30, 32, etc. (from air) at essentially zero and makes it quite sensitive to traces of gases in this range. Samples of hydrogen, helium, and argon to be used in experimental mixtures were scanned for low molecular weight impurities. Traces were found in each case at mass number 15 as well as those corresponding to air, but no other noticeable impurities below mass 30. The trace at mass 15 is attributed to methane from stopcock grease and the fact that cold traps were not used for sampling in these cases. The commercial carbon monoxide (referred to as tank CO) used in the experiments reported here was analysed on the Consolidated Mass Spectrometer Model 21-401. This instrument uses oil diffusion pumps and activated charcoal traps giving a relatively high background of hydrogen and low molecular weight hydrocarbon fragments, making observation of traces of these impurities difficult. However, it is estimated that, working in satisfactory pressure ranges, one can detect impurities of 0.02 mole per cent above background and this figure can be assigned as the sensitivity of hydrogen measurements. Scanning the region up to a mass number of thirty showed no significant increase over background except for the peaks at mass numbers 2, 14, 28 as expected. This gave for the hydrogen impurity in tank CO the value 0.82 ± 0.02 mole per cent.

EXPERIMENTAL RESULTS

Carbon monoxide-hydrogen mixtures

Six mixtures of varying composition of hydrogen in tank carbon monoxide were prepared and studied. Table I gives the results obtained from these measurements. These data have been plotted in Figure V giving for the intercept, $s = 1.09 \pm .08 \times 10^4 \text{ sec}^{-1}$, and for the slope, $m = 0.0205 \pm .0013 \times 10^4 \text{ sec}^{-1} \text{ atm}$. From this we have

$$\tau_a = 0.918 \pm .07 \times 10^{-4} \text{ sec.}$$

$$\tau_b = \frac{(0.0205) (10^{-4})}{(1.09)(1.11)} 1.69 \pm .20 \times 10^{-6} \text{ sec. atm.}$$

It can be seen in Appendix III that, at least for the mixtures with low hydrogen pressures, there will be some deviation from linearity for the phase shift given by $\phi = \tan^{-1} \frac{P}{\omega \tau_0}$. Assuming that the mixture richest in hydrogen has a relaxation time due entirely to hydrogen, and that τ_0 represents a good approximation for the relaxation time due to hydrogen, approximate corrections can be applied to the data for the nonlinear part of the curve and a more accurate determination can be made.

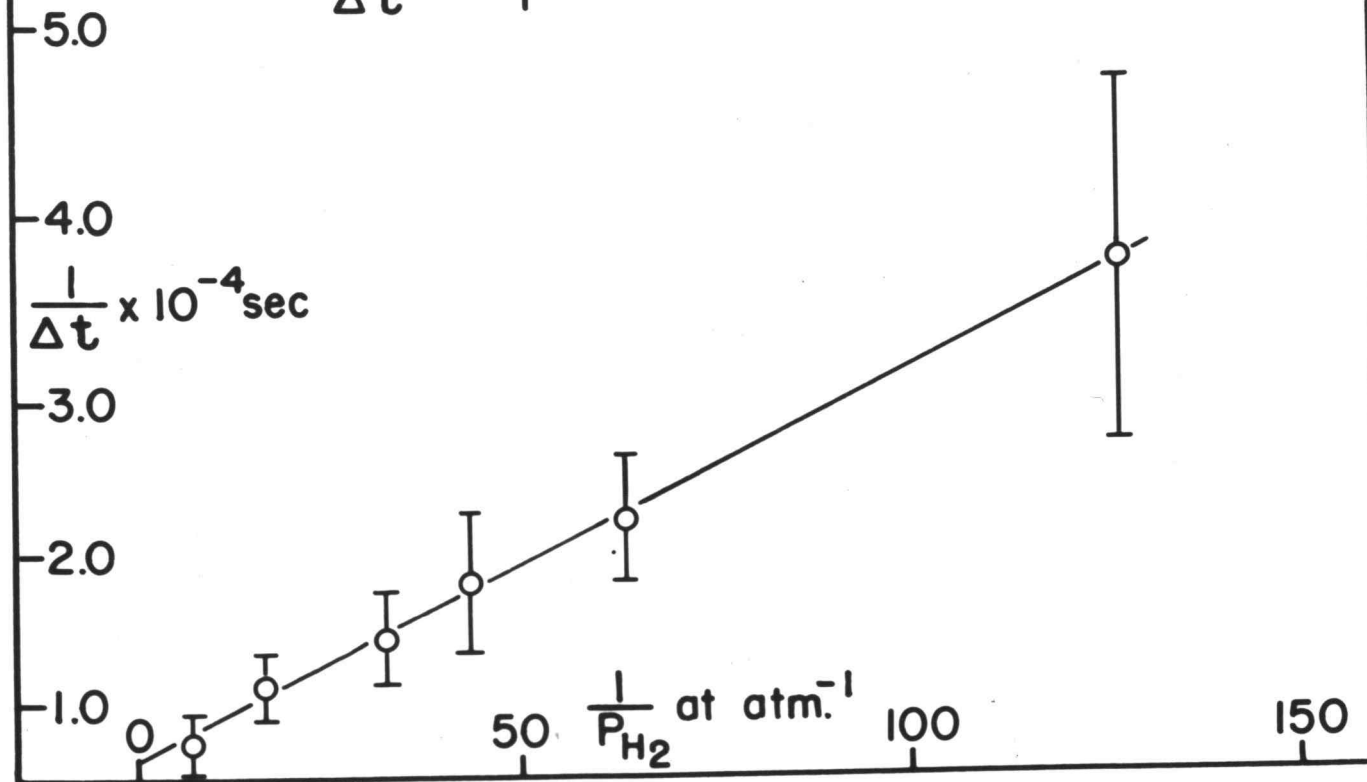
Knowing the amount of hydrogen in tank CO and carefully measuring the partial pressures of tank CO and hydrogen (or other diluent) in any given mixture, one can

TABLE I
 VIBRATIONAL RELAXATION MEASUREMENTS ON
 HYDROGEN-CARBON MONOXIDE MIXTURES

% hydrogen added to tank CO	3.02	6.01	2.31	1.58	0.785	13.45
Total % H ₂	3.82	6.78	3.11	2.39	1.599	14.16
1/P _b atm ⁻¹	33.1	16.6	43.3	63.3	127.4	7.44
	$\Delta t \times 10^4 \text{ sec.}$					
Trial 1	0.65	0.66	0.51	0.34	0.20	0.72
Trial 2	0.58	0.56	0.44	0.39	0.18	0.66
Trial 3	0.66	0.59	0.43	0.43	0.27	0.81
Trial 4	0.50	0.54	0.65	0.53	0.39	0.96
Trial 5	0.50	0.63	0.64	0.49	0.38	0.97
Trial 6	0.48	0.62	0.45	0.36	0.29	0.92
Trial 7	0.49	0.60	0.40	0.41	0.28	0.93
Trial 8	0.69	0.82	0.42	0.47	0.22	0.77
Trial 9		0.85	0.51	0.45	0.21	
Trial 10		0.85		0.36		
Trial 11				0.39		
$\Delta t \times 10^4$ sec.(average)	0.57	0.67	0.49	0.42	0.27	0.84
Standard deviation	± 0.08	± 0.08	± 0.09	± 0.06	± 0.07	± 0.11
1/ Δt sec. ⁻¹ $\times 10^{-4}$	1.75	1.49	2.04	2.38	3.71	1.19
Deviation	$\pm .25$	$\pm .18$	$\pm .37$	$\pm .34$	$\pm .96$	$\pm .16$

Fig. V
Carbon Monoxide-Hydrogen

$$\frac{1}{\Delta t} \text{ vs } \frac{1}{P}$$



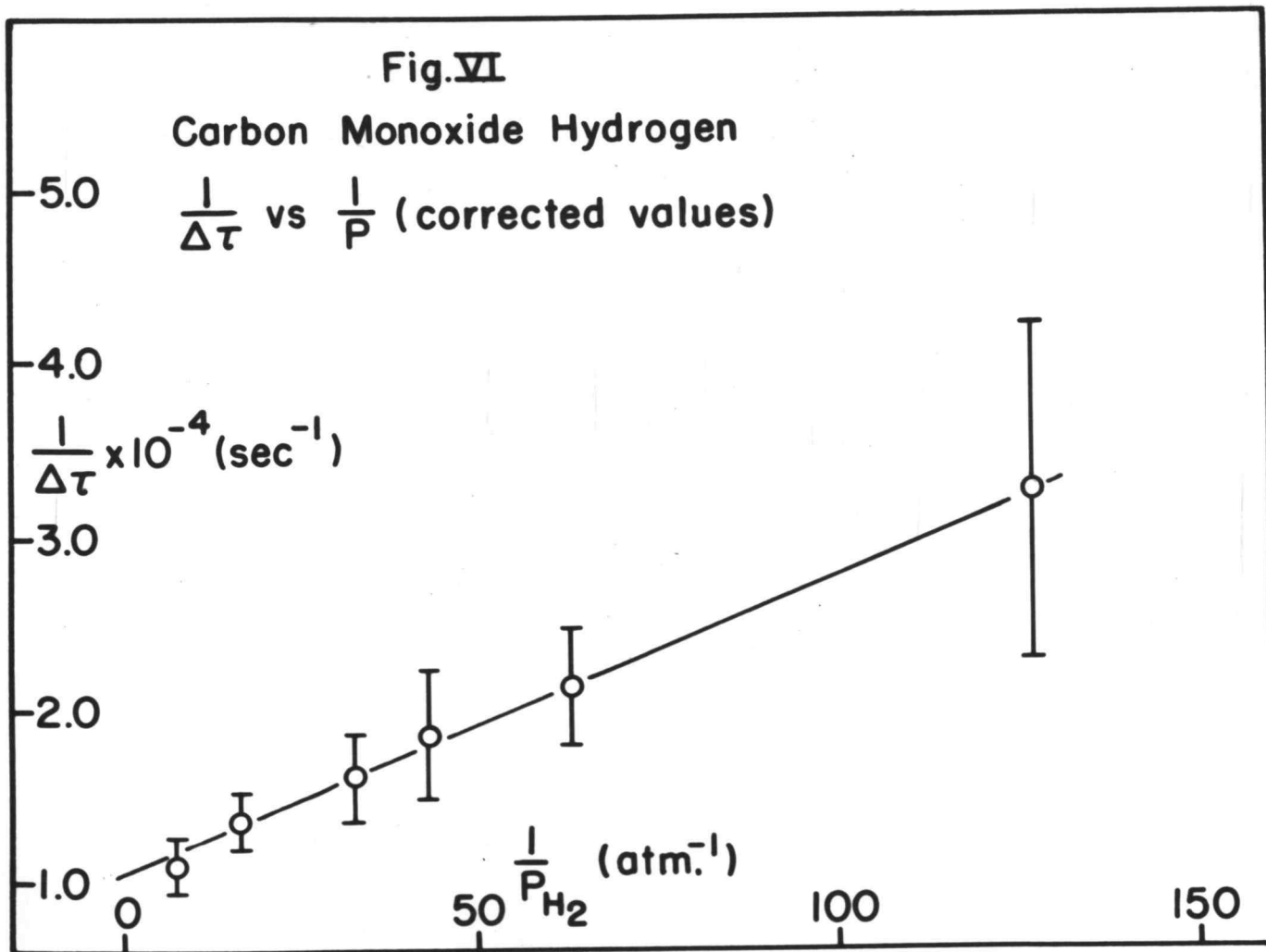
calculate the actual partial pressures of each significant gas in the mixture. In this way the partial pressures of hydrogen in the above series of measurements were found. This gives for the richest mixture a total of 14.16% hydrogen, and a relaxation time under the assumptions of the previous paragraph of $\tau = 0.119 \times 10^{-4}$ sec. and $t = 4.05 \times 10^{-4}$ sec. In Table II are tabulated the corresponding values of t , τ , $\Delta\tau$, and $1/\Delta\tau$ as interpolated from Figure VIII in Appendix III, for the six mixtures of hydrogen and tank carbon monoxide.

Figure VI shows the values of $1/\Delta\tau$, corrected for the nonlinearity of the arctangent function, plotted against $1/P_{H_2}$. The line represents a least squares fit to the $1/\Delta\tau$ values giving for the intercept, $s = 1.046 \pm .04 \times 10^4 \text{ sec.}^{-1}$ and for the slope, $m = 0.01725 \pm .00067 \times 10^4 \text{ sec.}^{-1} \text{ atm.}$ From this we obtain for the relaxation time of tank carbon monoxide $\tau_a = 1/s = 0.96 \pm 0.04 \times 10^{-4} \text{ sec.}$ and for the relaxation time of hydrogen-carbon monoxide collisions $\tau_b = \frac{m}{s(s+m)} = 1.55 \pm .10 \times 10^{-6} \text{ sec.}$ Knowing that tank carbon monoxide contains 0.82% hydrogen, the relaxation time of pure carbon monoxide can be estimated from the relaxation time of hydrogen, $\tau_b = 1.55 \times 10^{-6} \text{ sec. atm.}$ and the relaxation time of tank carbon monoxide, $\tau_a = 0.96 \times 10^{-4} \text{ sec.}$, by the relationship

TABLE II

CORRECTED VALUES OF $\Delta\tau$ AND $1/\Delta\tau$
FOR HYDROGEN-CARBON MONOXIDE MIXTURES

$1/P \text{ atm.}^{-1}$	$t \times 10^4 \text{ sec.}$	$\tau \times 10^4 \text{ sec.}$	$\Delta\tau \times 10^4 \text{ sec.}$	$1/\Delta\tau \times 10^{-4} \text{ sec.}^{-1}$
33.1	3.78	0.39	0.62	$1.61 \pm .25$
16.6	3.88	0.28	0.73	$1.37 \pm .18$
43.3	3.70	0.47	0.54	$1.85 \pm .37$
63.3	3.63	0.54	0.47	$2.13 \pm .34$
127.4	3.48	0.70	0.31	$3.23 \pm .96$
7.44	4.05	0.11	0.90	$1.11 \pm .16$
0	3.21	1.01		



$$\frac{1}{\tau_a} = \frac{P_b}{\tau_b} + \frac{P_{co}}{\tau_{co}}$$

$$\tau_{co} = \frac{P_{co}}{\frac{1}{\tau_a} - \frac{P_b}{\tau_b}} = 1.92 \pm .20 \times 10^{-4} \text{ sec. atm.}$$

Carbon monoxide-helium mixtures

Three mixtures of helium and tank carbon monoxide were prepared and their relaxation times measured by comparison with tank carbon monoxide taken as an absolute standard. Table III gives the results of these measurements.

Since the standard deviation in measured Δt values is fairly large, the agreement among the three determinations is considered quite good, and $\tau_{He} = 2.72 \pm .40 \times 10^{-6}$ sec. atm. is a reasonable value for the relaxation time resulting from carbon monoxide-helium collisions.

Carbon monoxide-neon mixture

Only one mixture of carbon monoxide and neon was prepared, since the reasonable agreement of measurements on mixtures of helium and carbon monoxide indicate that a fair value can thus be realized. Table IV records the experimental results from this determination.

TABLE III
 VIBRATIONAL RELAXATION DATA OF
 CARBON MONOXIDE-HELIUM MIXTURES

% helium	3.03	6.06	9.08
	$\Delta t \times 10^4$ sec.		
Trial 1	0.41	0.57	0.57
Trial 2	0.45	0.61	0.79
Trial 3	0.47	0.59	0.86
Trial 4	0.45	0.61	0.60
Trial 5	0.49	0.52	0.53
Trial 6	0.50	0.60	0.78
Trial 7	0.46	0.60	0.76
Trial 8	0.46	0.65	0.73
Trial 9			0.68
Trial 10			0.69
Trial 11			0.78
Trial 12			0.69
$\Delta t(\text{avg.}) \times 10^4$ sec.	0.46	0.59	0.70
Standard deviation	± 0.026	± 0.035	± 0.09
$\tau \times 10^4$ sec.	$0.46 \pm .05$	$0.33 \pm .05$	$0.22 \pm .10$
$\tau_{\text{He}} \times 10^6$ sec. atm.	$2.61 \pm .48$	$2.95 \pm .65$	2.53 ± 1.42
$\tau_{\text{He}}(\text{avg.}) \times 10^6$ sec. atm.	2.72 ± 0.40		

TABLE IV
 EXPERIMENTAL RESULTS
 CARBON MONOXIDE-NEON MIXTURE

% neon	$\Delta t \times 10^4$ sec.
	8.24
Trial 1	0.11
Trial 2	0.10
Trial 3	0.13
Trial 4	0.05
Trial 5	0.00
Trial 6	0.13
Trial 7	0.17
Trial 8	0.15
Trial 9	0.11
Trial 10	0.04
$\Delta t(\text{avg.}) \times 10^4$ sec.	0.10 ± 0.05
$\tau \times 10^4$ sec.	0.85 ± 0.06
$\tau_{\text{Ne}} \times 10^5$ sec. atm.	3.7 ± 1.1

Carbon monoxide-argon mixture

Here again only one mixture was prepared. The deviation of the relaxation time from that of tank carbon monoxide for argon and neon mixtures is so slight that there would be no significant variation of different mixtures and, hence, little further information to be gained. It must be realized that these measurements are subject to considerable error but at least the results are of the correct order of magnitude. Table V records the results of this measurement.

The effect of mass on the relaxation time

We now have what seem to be reasonable values for the relaxation time of the vibrational state of carbon monoxide in collisions with hydrogen, helium, and in self-collisions. Also, we have estimates of the relaxation time for collisions of carbon monoxide with neon and argon. In order to test the validity of the Schwartz-Slawsky-Herzfeld theory, the logarithm of these relaxation times will be plotted against the cube root of the reduced mass. Also, for comparison, the logarithm of the relaxation time will be plotted against the reduced mass itself. Table VI gives the values of the relaxation times and corresponding values of reduced mass.

TABLE V
 EXPERIMENTAL RESULTS
 CARBON MONOXIDE-ARGON MIXTURE

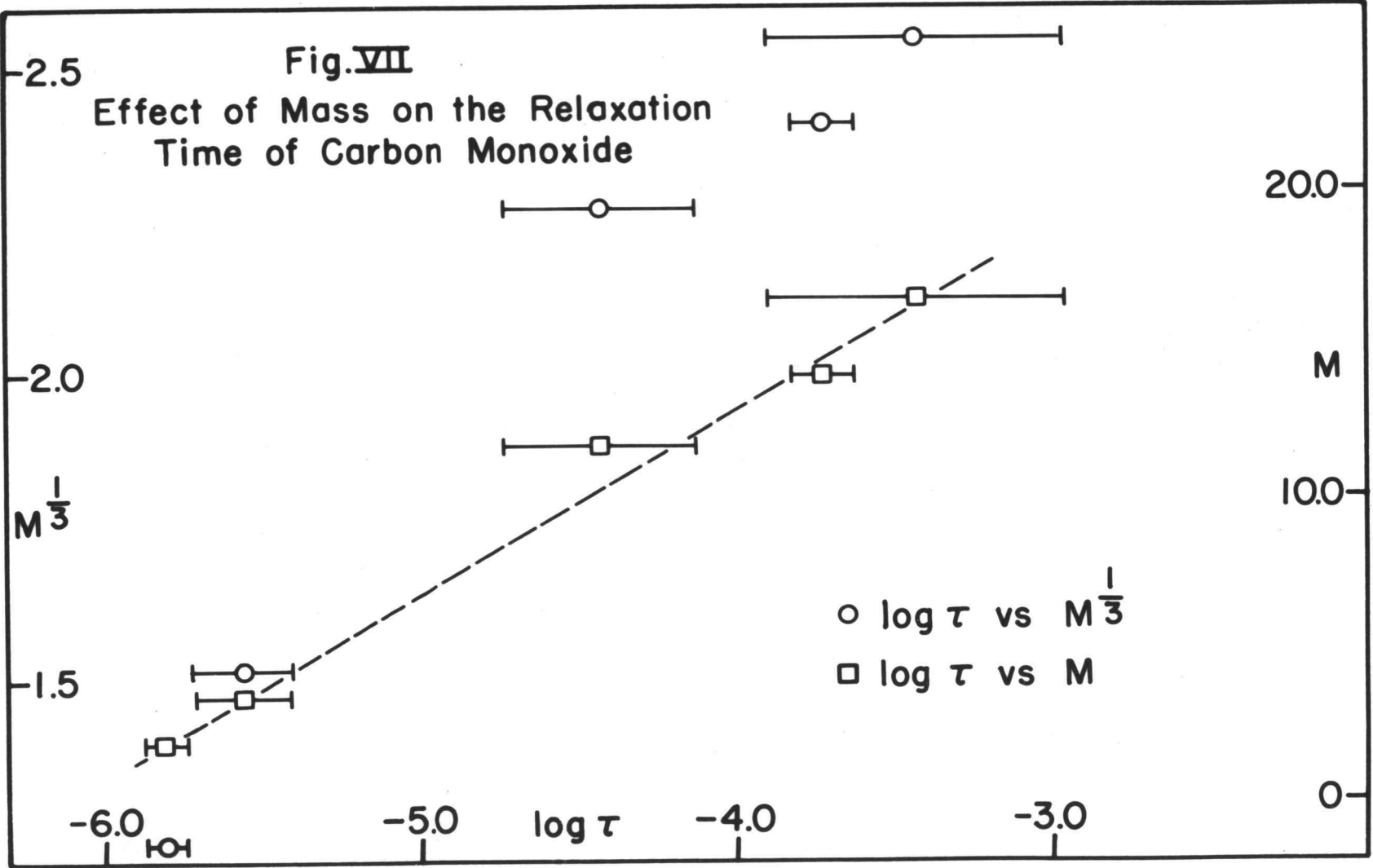
% argon	15.03
$\Delta t \times 10^4 \text{ sec.}$	
Trial 1	0.10
Trial 2	0.12
Trial 3	0.14
Trial 4	0.09
Trial 5	0.05
Trial 6	0.07
Trial 7	0.10
Trial 8	0.05
Trial 9	0.06
Trial 10	0.11
<hr/>	
$\Delta t \times 10^4 \text{ sec. (average)}$	-0.09
Standard deviation	± 0.027
$\tau \times 10^4 \text{ sec.}$	$1.08 \pm .05$
$\tau_A \times 10^4 \text{ sec. atm.}$	3.7 ± 1.7

TABLE VI
RELAXATION TIME AS A
FUNCTION OF REDUCED MASS

Type of collision	$\tau \times 10^4$ (sec. atm.)	$\log. \tau$	M (gm./mole)	$M^{1/2}$
CO-H ₂	0.0155	-5.81	1.87	1.23
CO-He	0.0270	-5.57	3.5	1.52
CO-Ne	0.37	-4.43	11.7	2.27
CO-CO	1.92	-3.72	14.0	2.41
CO-A	3.7	-3.43	16.5	2.55

Fig.VII

Effect of Mass on the Relaxation Time of Carbon Monoxide



This data is plotted in Figure VII both as a function of M and $M^{\frac{1}{3}}$. It is obvious at once that the relaxation time is very sensitive to collision mass but not nearly so sensitive as predicted by theory. It definitely rules out an energy of activation mechanism for this series of mixtures, which would predict no effect of mass on the relaxation time. It is interesting to note that a plot of logarithm τ against M seems to give a much better approximation to a straight line than does $M^{\frac{1}{3}}$.

CONCLUSIONS

The effect of various relaxing gases on the lifetime of the vibrational state of carbon monoxide has been determined with a view toward determining the influence of reduced collision mass on this process. It is believed that the values listed below in Table VII are fairly accurate for carbon monoxide-hydrogen, carbon monoxide-helium, and carbon monoxide-carbon monoxide collisions, while the values for carbon monoxide-neon and carbon monoxide-argon collisions are less certain, but of the correct order of magnitude. Also tabulated are the values for probability of deexcitation from the first vibrational level upon collision, $P_{1 \rightarrow 0}$.

As a comparison with other work, it may be noted that Sherratt and Griffiths (33) report a relaxation time of 1×10^{-5} sec. atm. for carbon monoxide for a temperature range from 1000° to 1800° Centigrade. At higher temperatures it is expected that the relaxation time would be shorter due to higher collision efficiency, so qualitatively this is in agreement. However, it is generally agreed and has been demonstrated that the relaxation time is a function of the temperature (9, 10, 11, 12, 24, 35), so that these results can be criticized on the basis of showing a constant relaxation time over

TABLE VII

RELAXATION TIME AND PROBABILITY OF DEEXCITATION
ON COLLISION FOR VARIOUS CARBON MONOXIDE MIXTURES

Type of collision	$\tau \times 10^4$ (calculated) (sec. atm.)	$\tau \times 10^4$ (experimental) (sec. atm.)	$P_{1 \rightarrow 0} \times 10^7$ (per collision)
CO-H ₂	.0087	0.0155	188.
CO-He	.0454	0.0270	159.
CO-Ne	16.0	0.37	20.
CO-CO	76.4	1.92	3.16
CO-A	123.	3.7	2.0

a wide temperature range. The only other reported measurement on the relaxation time of carbon monoxide is that of Turrell (38), his data having been taken at room temperature. He found for tank carbon monoxide a value of 6.2×10^{-5} seconds for τ . This carbon monoxide was subsequently analysed on the mass spectrometer and found to contain 1.67% hydrogen. The present values for τ_{Co} and τ_{H_2} give a predicted lifetime of 6.29×10^{-5} seconds for this gas. This is considered in excellent agreement with Turrell's measurement.

The mass dependence does not seem to follow the theory of Schwartz, Slawsky, and Herzfeld, but seems to fit better an exponential $\{-CM\}$ relationship. The predicted values for hydrogen and helium collisions are in fair agreement, especially since the simple one-dimensional model should appear more efficient than the three dimensional actuality. The use of the parameter α may give some insight into the fact that the theory does not predict the efficiency of larger reduced mass collisions. This term is essentially the slope of the potential energy curve at the classical point of closest approach under velocities comparable to the thermal average. Considerably higher velocities and, hence, closer approaches, are required for deexcitation in these large mass cases which makes the assumed values of α

somewhat naive. The larger slope would indicate the use of a larger value of α , which appears in the exponent to the minus two-thirds power. Thus, increasing α would increase the probability of deexcitation and decrease the relaxation time in correspondence with the observed values. In this respect it can be noted that, in the case of CO-A collisions, it would be sufficient to multiply α by four-thirds to bring the predicted value in line with the experimental value. Even smaller increases would suffice for CO-CO and CO-Ne collisions.

The relaxation time is very sensitive to the reduced mass which rules out a purely activation energy mechanism. It is felt, then, that no theory yet adequately describes the relaxation phenomena, especially in view of the apparent chemical efficiency of mixtures like carbon dioxide-water and hydrogen chloride-chlorine (8) as well as the structural efficiency found by McGrath and Ubbelohde (24).

In analysis of the data of this research it was found that many of the relaxation times fell in a region where the linear approximation of $\tan^{-1} 1/\omega\tau$ no longer held. For ease of analysis and maximum sensitivity it is desirable that this be avoided. Also, measurement of longer relaxation times, such as pure carbon monoxide, is extremely difficult if not impossible with any degree of

accuracy on this instrument because the relation $\omega\tau \ll 1$ no longer is maintained. An instrument using a much slower chopping frequency would prove highly desirable as it would give a much wider range for the determination of vibrational life-times.

Perhaps an even more profitable arrangement would be the design of a frequency response spectrophone. Since the signal amplitude is proportional to $1 / (1 + \omega^2\tau^2)^{\frac{1}{2}}$, if ω is varied the signal strength should fall off quite rapidly in the region where ω is approximately $1/\tau$. This would allow the determination of an absolute value of τ for each mixture without the need of complicated phase measuring apparatus.

BIBLIOGRAPHY

1. Amme, Robert and Sam Legvold. Excitation of vibrations in halo-methane gases. *Journal of Chemical Physics* 23:1960-1961. 1955.
2. Bauer, Ernest. Method of calculating cross sections for molecular collisions. *Journal of Chemical Physics* 23:1087-1094. 1955.
3. Bethe, H. A. and E. Teller. Aberdeen proving ground report X-117. Maryland, Aberdeen proving grounds, 1940. 54 p.
4. Bourgin, D. G. Sound absorption and velocity in mixtures. *Physical Review* 50:355-369. 1936.
5. Byers, Walter H. Specific heats of carbon tetrafluoride from supersonic measurements. *Journal of Chemical Physics* 11:348-350. 1943.
6. Curtiss, Charles F. and F. T. Adler. The scattering of atoms from diatomic molecules. *Journal of Chemical Physics* 20:249-256. 1952.
7. Eucken, A. and S. Aybar. Die Stossanregung intramolekularer Schwingungen in Gasen und Gasmischungen, VI. *Zeitschrift fur physikalische Chemie* 46B:195-211. 1940.
8. Eucken, A. and R. Becker. Der Ubergang von Translations- in Schwingungsenergie beim Zusammenstoss verschiedenartiger Molekeln auf Grund von Schalldispersionsmessungen. *Zeitschrift fur physikalische Chemie* 20B:467-473. 1933.
9. Eucken, A. and Rudolf Becker. Die Stossanregung intramolekularer Schwingungen in Gasen und Gasmischungen auf Grund von Schalldispersionsmessungen, I. *Zeitschrift fur physikalische Chemie* 27B:219-234. 1934.
10. Eucken, A. and Rudolf Becker. Die Stossanregung intramolekularer Schwingungen in Gasen und Gasmischungen auf Grund von Schalldispersionsmessungen, II. *Zeitschrift fur physikalische Chemie* 27B:235-262. 1934.

11. Eucken, A. and Rudolf Becker. Die Stossanregung intramolekularer Schwingungen in Gasen und Gasmischungen auf Grund von Schalldispersionsmessungen, III. Zeitschrift für physikalische Chemie 30B:85-112. 1935.
12. Eucken, A. and Rudolf Becker. Die Stossanregung intramolekularer Schwingungen in Gasen und Gasmischungen auf Grund von Schalldispersionsmessungen, IV. Zeitschrift für physikalische Chemie 36B:163-183. 1937.
13. Fogg, P. G. T., P. A. Hanks, and J. D. Lambert. Ultrasonic dispersion in Halo-methane vapours. Proceedings of the Royal Society 219A:490-499. 1953.
14. Griffith, Wayland. Vibrational relaxation times in gases. Journal of Applied Physics 21:1319-1325. 1950.
15. Griffith, Wayland. Vibrational energy lag in shock waves. Physical Review 87:234. 1952.
16. Herzfeld, K. F. and F. O. Rice. Dispersion and absorption of high frequency sound waves. Physical Review 31:691-695. 1928.
17. Hirshfelder, Joseph O., Charles F. Curtise, and R. Byron Byrd. Molecular theory of gases and liquids. New York, Wiley, 1954. 1219 p.
18. Huber, P. W. and Arthur Kantrowitz. Heat capacity lag measurements in various gases. Journal of Chemical Physics 15:275-284. 1947.
19. Jacox, Marilyn Esther. Collisional energy exchange in gases: Use of the Spectrophone for studying relaxation processes in carbon dioxide. Ph. D. thesis. Ithaca, New York, Cornell University, 1956. 199 numb. leaves.
20. Kantrowitz, Arthur. Heat capacity lag in gas dynamics. Journal of Chemical Physics 14:150-164. 1946.
21. Kneser, Hans D. Zur Dispersionstheorie des Schalles. Annalen der Physik 11:761-777. 1931.

22. Lambert, J. D. and J. S. Rowlinson. Ultrasonic dispersion in organic vapors. Proceedings of the Royal Society 204A:424-434. 1950.
23. Landau, L. and E. Teller. Zur Theorie der Schall-dispersion. Zeitschrift der Sowietunion 10:34-43. 1936.
24. McGrath, W. D. and A. R. Ubbelohde. The effect of molecular structure in vibrational relaxation in ethylene. Proceedings of the Royal Society 227A: 1-9. 1954.
25. National Research Council of the United States of America. International critical tables. New York, McGraw Hill, 1933. 7 vols.
26. Richards, William T. Supersonic phenomena. Reviews of Modern Physics 11:36-64. 1939.
27. Richardson, Edward Gick. Ultrasonic physics. New York, Elsevier, 1952. 285 p.
28. Rossing, Thomas D. and Sam Legvold. Collision excitation of molecular vibrations in halogen-substituted methanes. Journal of Chemical Physics 23:1118-1125. 1955.
29. Schwartz, Robert N. and Karl F. Herzfeld. Vibrational relaxation times in gases (three dimensional treatment). Journal of Chemical Physics 22:767-773. 1954.
30. Schwartz, R. N., Z. I. Slawsky, and K. F. Herzfeld. Calculation of vibrational relaxation. Journal of Chemical Physics 20:1591-1599. 1952.
31. Sette, D., A. Busala, and J. C. Hubbard. Energy transfer by collisions in cis- and trans-dichloro-ethylene vapors. Journal of Chemical Physics 20: 1899-1902. 1952.
32. Sette, D., A. Busala, and J. C. Hubbard. Energy transfer by collisions in vapors of chlorinated methanes. Journal of Chemical Physics 23:787-793. 1955.

33. Sherratt, G. B. and E. Griffiths. The determination of the specific heat of gases at high temperatures by the sound velocity method. I. Carbon monoxide. Proceedings of the Royal Society 147A:292-303. 1934.
34. Slobadskaya, P. V. Determination of the rate of transformation of molecular vibrational energy to translational energy by means of the spectrophone. Izvestilia akademiia nauk SSSR (seriia fizicheskaiia) 12:656-662. 1948.
35. Smiley, Edward F. and Ernest H. Winkler. Shock-tube measurements of vibrational relaxation. Journal of Chemical Physics 22:2018-2022. 1954.
36. Smiley, E. F., E. H. Winkler, and Z. I. Slawsky. Measurement of the vibrational relaxation effect in CO₂ by means of shock tube interferograms. Journal of Chemical Physics 20:923-924. 1952.
37. Stepanov, P. E. Relaxation phenomena in a shock wave in a gas. Journal of Experimental and Theoretical Physics (USSR) 17:377-385. 1947.
38. Turrell, George Charles. Determination of the vibrational lifetime of carbon monoxide by the spectrophone method. Ph. D. thesis. Corvallis, Oregon State College, 1954. 82 numb. leaves.
39. van Itterbeek, A. and P. Mariens. Measurements on the velocity and absorption of sound in various gases between 100° C. and -100° C. Influence of pressure on the absorption. Physika 4:609-616. 1937.
40. Widom, Benjamin and S. H. Bauer. Energy exchange in molecular collisions. Journal of Chemical Physics 21:1670-1685. 1953.
41. Zener, Clarence. Interchange of translational, rotational, and vibrational energy in molecular collisions. Physical Review 37:556-569. 1931.
42. Zener, Clarence. Low velocity inelastic collisions. Physical Review 38:277-281. 1931.

APPENDIXES

APPENDIX I

In order to evaluate the Schwartz-Slawsky-Herzfeld theory for the gas mixtures to be studied, the vibrational relaxation times for one atmosphere of relaxing gas will be calculated for hydrogen, helium, neon, carbon monoxide, and argon. This series of gases has been selected so that only carbon monoxide will be infrared active, that is, absorb infrared radiation, and, hence, the occurrence of a pressure signal in the cell must result from collision of carbon monoxide molecules with other gas molecules. To complete the calculation we determine the exponential behavior, σ ; the matrix element for the transition from the first vibrational quantum level to the ground state, V_1 ; the probability of such vibrational energy loss with corresponding increase in the translational energy, $P_{1 \rightarrow 0}$; the total number of collisions per second per atmosphere of relaxing gas $M_{a,b}$; and finally the relaxation time for one atmosphere of relaxing gas, τ_0 . Values of the Lennard-Jones potential constant, r_0 , were obtained from Hirshfelder, Curtiss and Byrd (17, pl111). The results are given in Table VIII.

In order to test the validity of approximations made in the derivation of this theory, Table IX gives the values of quantities necessary to evaluate the inequalities $\exp \left\{ \frac{4 \pi^2 M v_0^*}{\alpha h} \right\} \gg 1$; $v_0^* \gg \left(\frac{2 \Delta E}{M} \right)^{\frac{1}{2}}$

TABLE VIII

THEORETICAL CALCULATION OF RELAXATION
TIMES FOR CARBON MONOXIDE MIXTURES

Relaxing gas	$r_0(\text{A})$	σ	$V_i \times 10^2$	$P_{1 \rightarrow 0}$ per collision	$M_{a,b} \times 10^{-10}$ collisions/sec.	τ_0 sec. atm.
CO	3.763	33.40	1.97	1.23×10^{-12}	1.65	49.0
H ₂	3.279	12.79	2.60	3.46×10^{-5}	3.44	8.40×10^{-7}
He	3.160	16.44	2.80	3.08×10^{-5}	2.33	1.40×10^{-6}
Ne	3.256	27.78	2.63	2.14×10^{-10}	1.36	0.344
A	3.584	34.77	2.17	4.06×10^{-13}	1.36	181.

TABLE IX

EVALUATION OF QUANTITIES FOUND IN
INEQUALITIES IN DEVELOPMENT OF THEORY

Type of collision	$\left(\frac{2\Delta E}{M}\right)^{\frac{1}{2}} \times 10^{-5}$ (cm./sec.)	$v_0^* \times 10^{-5}$ (cm./sec.)	$\frac{4\pi^2 M v_0^*}{\alpha h}$
CO-CO	1.92	1.44	42.9
CO-He	3.84	2.16	13.5
CO-A	1.74	1.32	45.9
CO-H ₂	5.26	2.69	9.3
CO-Ne	2.10	1.46	31.3

The results indicate that for any but the lightest molecules the relaxation times would be extremely long. It must be pointed out that such long relaxation times, even if they existed, could not be measured since trace low molecular weight impurities as well as wall effects would limit the length of time observable as, indeed, would the finite time before re-radiation. However, it must be remembered that approximations made in this theory are not valid for high energy transitions as occur in carbon monoxide. In any event, the relaxation times would be expected to be much shorter than those calculated here for high molecular weight collisions.

APPENDIX II

It is the purpose of this section to evaluate the heat conduction phase shift and compare it with the values of $\omega\tau$ observed experimentally. The expression for this term is

$$\tan \bar{\phi} = \frac{\sum_{n=1}^{\infty} \sum_{m=1}^{\infty} \frac{1}{n^2} \frac{1}{\lambda_m^2} \frac{1 + \frac{\delta_{m,n}}{\delta_{m,n}^2}}{1 + \frac{\delta_{m,n}}{\delta_{m,n}^2}}}{\sum_{n=1}^{\infty} \sum_{m=1}^{\infty} \frac{1}{n^2} \frac{1}{\lambda_m^2} \frac{1}{1 + \frac{\delta_{m,n}}{\delta_{m,n}^2}}} \quad (n \text{ odd})$$

$$\delta_{m,n} = \frac{k}{c \omega} \left(\frac{n^2 \pi^2}{L^2} + \frac{\lambda_m^2}{a^2} \right)$$

Because $\frac{k}{c \omega}$ is very small, approximately 10^{-5} cm^2 , it is only for very large values of m and n that the value of $\delta_{m,n}$ compares with 1. Thus, it can be seen that the sum in the denominator has converged to a fair approximation before $\delta_{m,n}^2$ presents an appreciable contribution. This makes possible the approximation

$$\begin{aligned} \sum_{n=1}^{\infty} \sum_{m=1}^{\infty} \frac{1}{n^2} \frac{1}{\lambda_m^2} \frac{1}{1 + \frac{\delta_{m,n}}{\delta_{m,n}^2}} &\approx \sum_{n=1}^{\infty} \sum_{m=1}^{\infty} \frac{1}{n^2} \frac{1}{\lambda_m^2} \\ &= \sum_{n=1}^{\infty} \frac{1}{n^2} \sum_{m=1}^{\infty} \frac{1}{\lambda_m^2} = U \cdot V \end{aligned}$$

where $U = \sum_{n=1}^{\infty} \frac{1}{n^2} = \frac{\pi^2}{8}$ for n odd.

$$V = \sum_{m=1}^{\infty} \frac{1}{\lambda_m^2} = \frac{1}{4}$$

The numerator in the above expression can be

expressed as two sums

$$\sum_{n=1}^{\infty} \sum_{m=1}^{\infty} \frac{1}{n^2} \frac{1}{\lambda_m^2} \frac{\delta_{m,n}}{1 + \delta_{m,n}^2} = I + II \text{ where}$$

$$I = \sum_{n=1}^{\infty} \sum_{m=1}^{\infty} \frac{k}{\omega c} \frac{\pi^2}{L^2} \frac{1}{\lambda_m^2} \frac{1}{1 + \delta_{m,n}^2};$$

$$II = \sum_{n=1}^{\infty} \sum_{m=1}^{\infty} \frac{k}{\omega c} \frac{1}{a^2} \frac{1}{n^2} \frac{1}{1 + \delta_{m,n}^2}$$

In I we see from the previous argument that for all values of δ_m that make a significant contribution to $\frac{1}{1 + \delta_{m,n}^2}$ the series has already converged to a fair approximation. Thus I can be written

$$I \approx \frac{k}{\omega c} \frac{\pi^2}{L^2} \sum_{m=1}^{\infty} \frac{1}{\lambda_m^2} \sum_{n=1}^{\infty} \frac{1}{1 + \left(\frac{k}{\omega c}\right)^2 \frac{\pi^4}{L^4} n^4} \quad (n \text{ odd})$$

Similarly, II is given by

$$II \approx \frac{k}{\omega c} \frac{1}{a^2} \sum_{n=1}^{\infty} \frac{1}{n^2} \sum_{m=1}^{\infty} \frac{1}{1 + \left(\frac{k}{\omega c}\right)^2 \frac{1}{a^4} \lambda_m^4} \quad (n \text{ odd})$$

The first sums are known in either case and it remains to evaluate the latter sums.

$$\text{Consider the sum } \sum_{n=1}^{\infty} \frac{1}{1 + \left(\frac{k}{\omega c}\right)^2 \frac{\pi^4}{L^4} (2\ell - 1)^4} \quad (n \text{ odd})$$

$$= \sum_{\ell=1}^{\infty} \frac{1}{1 + \left(\frac{k}{\omega c}\right)^2 \frac{\pi^4}{L^4} (2\ell - 1)^4} = \frac{1}{2} \sum_{\ell=-\infty}^{\infty} \frac{1}{1 + \left(\frac{k}{\omega c}\right)^2 \frac{\pi^4}{L^4} (2\ell - 1)^4}$$

The term $\left(\frac{k}{\omega c}\right)^2 \frac{\pi^4}{L^4} (2\ell - 1)^4$ varies only very slowly

with ℓ , and can be fitted quite closely by a function continuous in ℓ .

$$\sum_{\ell=-\infty}^{\infty} \frac{1}{1 + \left(\frac{k}{\omega c}\right)^2 \frac{\pi^4}{L^4} (2\ell - 1)^4} \approx \int_{-\infty}^{+\infty} \frac{1}{1 + \left(\frac{k}{\omega c}\right)^2 \frac{\pi^4}{L^4} (2\ell - 1)^4} d\ell$$

$$\text{Let } x = \left(\frac{k}{\omega c}\right)^{\frac{1}{2}} \frac{\pi}{L} 2\ell \quad ; \quad x_0 = \left(\frac{k}{\omega c}\right)^{\frac{1}{2}} \frac{\pi}{L}$$

$$\sum_{\ell=-\infty}^{\infty} \frac{1}{1 + \left(\frac{k}{\omega c}\right)^2 \frac{\pi^4}{L^4} (2\ell - 1)^4} \approx \left(\frac{\omega c}{k}\right)^{\frac{1}{2}} \frac{L}{2\pi} \int_{-\infty}^{+\infty} \frac{dx}{1 + (x - x_0)^4}$$

The integral $\int_{-\infty}^{+\infty} \frac{dx}{1 + (x - x_0)^4}$ is readily evaluated by the method of residues to give

$$\int_{-\infty}^{+\infty} \frac{dx}{1 + (x - x_0)^4} = \frac{\pi}{\sqrt{2}}$$

$$\text{and } \sum_{n=1}^{\infty} \frac{1}{1 + \left(\frac{k}{\omega c}\right)^2 \frac{\pi^4}{L^4} n^4} \approx \frac{1}{2} \left(\frac{\omega c}{k}\right)^{\frac{1}{2}} \frac{L}{2\pi} \frac{\pi}{\sqrt{2}}$$

$$\text{Thus } I \approx \left(\frac{k}{\omega c}\right)^{\frac{1}{2}} \frac{\pi^2}{L} \frac{1}{4\sqrt{2}} V$$

The remaining sum can be evaluated in a similar manner if it is pointed out that for larger values of m , λ_m differs from $\pi(m - \frac{1}{4})$ by an arbitrarily small amount, and that it is only the larger values of λ_m that affect the sum significantly. Thus we have

$$\sum_{m=1}^{\infty} \frac{1}{1 + \left(\frac{k}{\omega c}\right)^2 \frac{1}{a^4} \lambda_m^4} \approx \sum_{m=1}^{\infty} \frac{1}{1 + \left(\frac{k}{\omega c}\right)^2 \frac{\pi^4}{a^4} \left(m - \frac{1}{4}\right)^4}$$

$$= \sim \frac{1}{2} \sum_{m=-\infty}^{\infty} \frac{1}{1 + \left(\frac{k}{\omega c}\right)^2 \frac{\pi^4}{a^4} \left(m - \frac{1}{4}\right)^4}$$

Where before
$$\sum_{\ell=1}^{\infty} \frac{1}{1 + \left(\frac{k}{\omega c}\right)^2 \frac{\pi^4}{L^4} (2\ell-1)^4} \equiv \frac{1}{2} \sum_{\ell=-\infty}^{\infty} \frac{1}{1 + \left(\frac{k}{\omega c}\right)^2 \frac{\pi^4}{L^4} (2\ell-1)^4}$$

it is not exactly correct to extend the sum over m to $\frac{1}{2}$ the sum from $-\infty$ to $+\infty$. However, it is only for small values of m that $(m - \frac{1}{4})^4$ differs appreciably from $(-m - \frac{1}{4})^4$ and the value of such terms in the sum is essentially unity — independent of m . Hence, the approximation of treating the function as symmetrical about the origin is justified.

This sum is readily approximated in a manner similar to the previous one to give

$$\sum_{m=1}^{\infty} \frac{1}{1 + \left(\frac{k}{\omega c}\right)^2 \frac{1}{a^4} \lambda_m^4} = \sim \left(\frac{\omega c}{k}\right)^{\frac{1}{2}} \frac{a}{\pi} \frac{1}{2} \cdot \frac{\pi}{\sqrt{2}} \text{ and}$$

$$II = \sim \left(\frac{k}{\omega c}\right)^{\frac{1}{2}} \frac{1}{a^2 \sqrt{2}} U$$

Combining terms for the heat conduction phase shift gives

$$\tan \bar{\phi} = \frac{\left(\frac{k}{\omega c}\right)^{\frac{1}{2}} \frac{\pi^2}{L} \frac{1}{4\sqrt{2}} V + \left(\frac{k}{\omega c}\right)^{\frac{1}{2}} \frac{1}{a^2 \sqrt{2}} U}{V \cdot U}$$

$$= \left(\frac{k}{\omega c}\right)^{\frac{1}{2}} \frac{1}{\sqrt{2}} \left[\frac{\pi^2}{4L} \frac{1}{U} + \frac{1}{2a} \frac{1}{V} \right]$$

$$= \left(\frac{2k}{\omega c}\right)^{\frac{1}{2}} \left[\frac{1}{L} + \frac{1}{a} \right]$$

It remains to show numerically that the inequalities

$$\omega\tau > \left(\frac{2k}{\omega c}\right)^{\frac{1}{2}} \left[\frac{1}{L} + \frac{1}{a}\right] \text{ and } \omega\tau \gg \frac{k\kappa^2}{\omega c} \text{ are satisfied.}$$

The required numerical values are, for this cell and carbon monoxide

$\omega = 3.77 \times 10^3$ radians/sec.; $k = 2.15 \times 10^{-4}$ Joules/degree cm. sec.; $C = 20.69$ Joules/degree gm. mole; $\rho = 1.25$ gm./liter; $M = 28$ gm./mole; $L = 7.62$ cm.; $a = 1.27$ cm.; $\kappa = \sim 0.08$ cm⁻¹. Here the heat capacity /cc is given by $c = \frac{C\rho}{M}$.

Using these values we find

$$\left(\frac{2k}{\omega c}\right)^{\frac{1}{2}} \left[\frac{1}{L} + \frac{1}{a}\right] = \sim 1.02 \times 10^{-2}$$

which corresponds to an observed time shift of 2.7μ seconds. What is actually measured is the variation in phase shift with variation in gas constituency. Since the total pressure remains at one atmosphere the heat conduction effect could not vary by more than a factor of two, or that 2.7μ seconds represents an upper limit to this variation. The observed shifts all corresponded to from ten to a hundred times this figure, and can only be accounted for by relaxation phenomena. Indeed the smallest value of $\omega\tau$ observed was 4.1×10^{-2} so that the relation

$$\omega\tau > \left(\frac{2k}{\omega c}\right)^{\frac{1}{2}} \left[\frac{1}{L} + \frac{1}{a}\right]$$

is satisfied.

Further, $\frac{k\kappa^2}{\omega c} \approx 4 \times 10^{-7}$, which, even for relaxation times on the order of μ seconds is such that $\omega\tau \gg \frac{k\kappa^2}{\omega c}$.

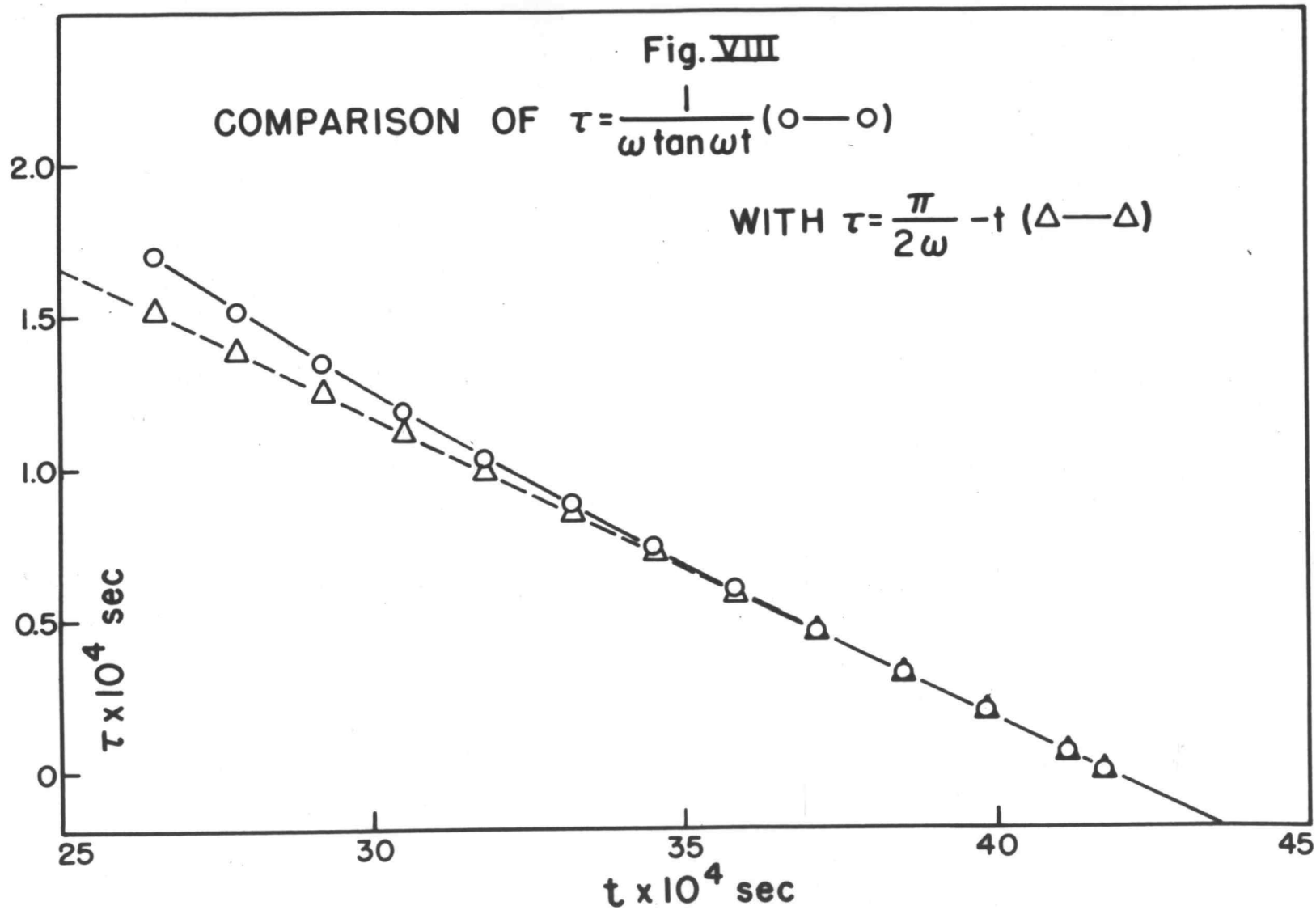
APPENDIX III

It will be necessary to determine the limits of validity of the linear approximation, $\tan^{-1} \frac{1}{\omega\tau} \approx \frac{\pi}{2} - \omega\tau$. In Figure VIII, $\tau = \frac{1}{\omega \tan \omega t}$ and $\tau = \frac{\pi}{2\omega} - t$ are plotted as a function of t , the observed time shift. In this way the validity of the linear approximation can be quickly checked and a suitable correction factor applied where necessary. Table X gives the calculated results that appear on the graph.

TABLE X

CALCULATION OF $\tau = \frac{1}{\omega \tan \omega t}$ AND $\tau = \frac{\pi}{2\omega} - t$

$t \times 10^4$	ωt	$\tan \omega t$	$\frac{1 \times 10^4}{\omega \tan \omega t}$	$\frac{\pi}{2\omega} - t \times 10^4$
4.17	1.57		0	0
4.11	1.55	48.08	.06	.06
3.98	1.50	14.10	.19	.19
3.85	1.45	8.238	.32	.32
3.71	1.40	5.798	.46	.46
3.58	1.35	4.455	.60	.59
3.45	1.30	3.602	.74	.72
3.32	1.25	3.010	.88	.85
3.18	1.20	2.572	1.03	.99
3.05	1.15	2.234	1.19	1.12
2.92	1.10	1.965	1.35	1.25
2.78	1.05	1.743	1.52	1.39
2.65	1.00	1.557	1.70	1.52



APPENDIX IV

It is the purpose of this section to derive a useful expression for analysis of data obtained by means of the spectrophone. In every case a gas of unknown relaxation time is diluted with another gas to be studied, while the total pressure is maintained at 1 atmosphere. For such a mixture the combined relaxation time is given by

$$\frac{1}{\tau} = \frac{P_a}{\tau_a} + \frac{P_b}{\tau_b} \quad \text{where } P_a + P_b = 1. \quad \text{Here either gas}$$

'a', gas 'b' or both can be mixtures. Thus in analysis of CO-H₂ mixtures, 'b' is hydrogen while 'a' is tank carbon monoxide containing 0.82% hydrogen. Since absolute values of τ cannot be measured directly, it is necessary to consider an arbitrary time, t , that differs from τ by some constant factor, c . Then

$$t - c = \tau = \frac{1}{\frac{P_a}{\tau_a} + \frac{P_b}{\tau_b}} = \frac{1}{\frac{1}{\tau_a} + \left(\frac{1}{\tau_b} - \frac{1}{\tau_a}\right)P_b}$$

If now in each case the measured time is compared with that of the pure gas, a, we obtain the expression, where gas b is more efficient than gas a:

$$\Delta t = \tau_a \left(\frac{1}{\tau_b} - \frac{1}{\tau_a} \right) P_b \frac{1}{\frac{1}{\tau_a} + \left(\frac{1}{\tau_b} - \frac{1}{\tau_a} \right) P_b}$$

$$\frac{1}{\Delta t} = \frac{1}{\tau_a^2} \frac{1}{\frac{1}{\tau_b} - \frac{1}{\tau_a}} \frac{1}{P_b} + \frac{1}{\tau_a}$$

Then, if $\frac{1}{\Delta t}$ is plotted against $\frac{1}{P_b}$, the intercept is given by $s = \frac{1}{\tau_a}$ and the slope by $m = \frac{1}{\tau_a^2} \frac{1}{\frac{1}{\tau_b} - \frac{1}{\tau_a}} = \frac{s^2}{\frac{1}{\tau_b} - s}$

$$\text{This gives } \tau_a = \frac{1}{s} \qquad \tau_b = \frac{m}{s(s+m)}$$

Once this analysis has been carried out accurately for a given gas, a, it can serve as an absolute calibration for this gas in all other mixtures being studied.